Avdelningen för Konstruktionsteknik
Lunds Tekniska Högskola
Box 118
221 00 LUND

Division of Structural Engineering
Faculty of Engineering, LTH
P.O. Box 118
S-221 00 LUND
Sweden

Analysis of Jointless Bridges due to Horizontal Actions and Soil-Structure Interaction

Analys av skarvfria broar på grund av horisontella krafter och jord-konstruktion-samverkan

Pontus Christensson

2016

Rapport TVBK-5251

ISSN 0349-4969
ISRN: LUTVDG/TVBK-16/5251 (93)

Examensarbete 30 hp

Handledare: Oskar Larsson, Avd. Konstruktionsteknik, Erik Gottsäter, Avd. Konstruktionsteknik, Tore Nilsson, Tyréns AB

Juni 2016

ABSTRACT

Bridges constructed without joints function to take care of forces by introducing bending moments to the stiff connections. Jointless bridges, also called integral bridges, in different appearances are built all over the world, and are popular due to their advantages regarding life cycle cost. Usually the dimensions of the structural parts, especially the backwalls, tends to be large and the elements are heavily reinforced. By crediting the interaction between a bridge and the surrounding soil in the design work, material can be saved. Soil-structure interaction is a complex phenomenon where the boundary between soil and bridge may be modelled as springs with the same stiffness as the soil. The dissertation studies a method of FE modelling of the deformations and section forces, and also the extent of the soil-structure interaction, by introducing linear springs at the surface between soil and structure.

The work is carried out by investigating two bridges, one fully integrated abutment bridge and one bridge with backwalls (*sv. ändskärmsbro*). The bridges are solely loaded by horizontal forces, e.g. braking forces, temperature movements and earth pressure. An initial stiffness of the soil is chosen, and from there, with some help from measurement data, the results from the FE model has then been compared to both calculations of a simple load case, as well as measured data, to find the proper soil stiffness.

It is found that no sufficiently good convergence of the stiffness can be found from the measurement data, but the method shows good potential of working if more and more detailed analyses are made.

Keywords: *Jointless bridges, integrated abutment bridges, backwall, soil-structure interaction, FE modelling*

SAMMANFATTNING

Broar som konstrueras utan kopplingar och lager fungerar så att de ska ta upp krafter via moment i ramhörn eller liknande. Integrerade broar i olika utformningar byggs över hela världen, och är populära på grund av dess enkla utformning och fördelar rörande livscykelkostnader. Vanligtvis tenderar dimensionerna, då i synnerhet ändskärmarna, att bli väldigt tunga och tungt armerade. Genom att tillgodoräkna sig interaktionen mellan jord och konstruktion kan man minska momenten, och således också dimensionerna. Jord-konstruktion-interaktion är ett komplext fenomen där man till exempel kan modellera kontaktytan med ett fjädrande upplag, som innehar samma styvhet som jorden. Avhandlingen undersöker modelleringsmetoden genom att jämföra förskjutningar och moment för olika lastfall, och genom att jämföra både en beräkningsmodell genom ett simpelt lastfall samt mätdata från horisontella rörelser i en verklig bro.

Två broar undersöks, en bro med fullt integrerat landfäste samt en ändskärmsbro, och broarna är enbart belastade i horisontalled. Exempel på laster som kan påverka broarna är bromskraft från trafikerande bilar, temperaturförändringar eller jordtrycket som omgivande jord påverkar ändskärmen med. En initialstyvhet definieras och med hjälp av förskjutningarna givna av mätdata kan sedan rätt styvhet på jorden i FE-modellen hittas.

Det framgår av undersökningarna att ingen tillräckligt bra styvhet kan hittas för given metod, men att detta troligtvis är möjligt om hänsyn tas till de osäkerheter och fel som har identifierats.

PREFACE

The dissertation and the research in the dissertation was carried out in collaboration between Tyréns AB in Malmö and the Division of Structural Engineering at Lund University of Technology.

I would like to thank Oskar Larsson and Erik Gottsäter at the Division of Structural Engineering at Lund University of Technology for all the support throughout the project, and for all the valuable ideas provided.

I would also like to thank Tore Nilsson at the Division of Bridge Construction at Tyréns AB in Malmö, who has provided a lot of support and guidance, and showed a big interest for my work.

I am very grateful to the whole Division of Bridge Construction at Tyréns AB for all the help and support, especially to Björn for all the help with the models set up in Brigade. I will also show my gratitude towards Scanscot Technology AB for providing a license for Brigade/Plus as well as valuable help and knowledge with the model.

Lastly a big thank you to my beloved family and all my friends who is always there and have supported me throughout the years at the university.

Malmö, May 2016

Pontus Christensson

NOTATIONS

E	Young's modulus	$[N/m^2]$
E_c	Young's modulus of concrete	$[N/m^2]$
F	Concentrated load	$[N]$
H_{bw}	Height of backwall	$[m]$
K	Earth pressure coefficient	$[-]$
K_0	At rest earth pressure coefficient	$[-]$
K_a	Active earth pressure coefficient	$[-]$
K_p	Passive earth pressure coefficient	$[-]$
L_{exp}	Expansion length of bridge	$[m]$
M	Bending moment	$[Nm]$
M_{UDL}	Bending moment at the top of the backwall from uniformly distributed earth pressure	$[Nm]$
M_{NUDL}	Bending moment at the top of the backwall from non-uniformly distributed earth pressure	$[Nm]$
T_{max}	Maximum air temperature	$[°C]$
T_{min}	Minimum air temperature	$[°C]$
ΔT	Temperature difference	$[°C]$
c	Cohesion of the backfill soil	$[-]$
c_1	Constant depending on favourable or unfavourable conditions of loading	$[-]$
k	Spring stiffness	$[N/m]$
k_{init}	Initial spring stiffness of the backfill soil	$[N/m]$
k_s	Predicted spring stiffness of the backfill soil	$[N/m]$
k_{T1}	Spring stiffness at the western backwall (T1)	$[N/m]$
k_{T4}	Spring stiffness at the eastern backwall (T4)	$[N/m]$
p	Earth pressure	$[N/m^2]$
p_0	At rest earth pressure	$[N/m^2]$
p_1	$p_p - p_0$	$[N/m^2]$
p_p	Passive earth pressure	$[N/m^2]$
$p_{B,crane,bottom}$	Earth pressure of braking force at the bottom of the backwall due to braking of the crane	$[N/m^2]$
$p_{B,TRVK,bottom}$	Earth pressure of breaking force at the bottom of the backwall with braking force from TRVK	$[N/m^2]$
$p_{bf,bottom}$	Earth pressure of backfill soil at the bottom of the backwall	$[N/m^2]$
$p_{SL,bottom}$	Earth pressure of surcharge load at the bottom of the backwall	$[N/m^2]$
$p_{T,EC,bottom}$	Earth pressure of temperature movements at the bottom of the backwall with temp. diff. from Eurocode	$[N/m^2]$
$p_{T,meas,bottom}$	Earth pressure of temperature movements at the bottom of the backwall with temp. diff. from measurements	$[N/m^2]$

Δp	Earth pressure difference	$[N/m^2]$
q	Uniformly distributed load	$[N/m]$
$q_{resisting}$	Uniformly distributed resisting load of the breaking force	$[N/m]$
t	Thickness of backwall	$[m]$
v	Acceleration of the crane	$[m/s^2]$
z	Depth in soil	$[m]$
α	Angle of leaning surface	[°]
$\alpha_{\Delta T}$	Expansion coefficient for temperature	$[-]$
δ	Displacement	$[m]$
$\delta_{B,lim}$	Limit displacement of the braking crane	$[m]$
δ_{T1}	Displacement of the western backwall (T1)	$[m]$
δ_{T4}	Displacement of the eastern backwall (T4)	$[m]$
δ_{brake}	Displacement of the eastern backwall due to braking of the crane	$[m]$
$\varepsilon_{\Delta T}$	Temperature strain	$[-]$
ϕ'	Internal friction angle	[°]
γ	Self-weight of soil	$[N/m^3]$
ν	Poisson's ratio	$[-]$
σ_1	Principal stress in vertical direction	$[N/m^2]$
σ_2	Principal stress in radial direction	$[N/m^2]$
σ_3	Principal stress in radial direction	$[N/m^2]$
τ_{xy}	Shear stress	$[N/m^2]$

Indices

B	Braking
bf	Backfill soil
SL	Surcharge load
T	Temperature

ABBREVIATIONS

CTH	Chalmers University of Technology
EC	Eurocode
EPC	Earth Pressure Cell
FE	Finite element
KTH	Royal Institute of Technology
LTH	Lund University of Technology
LTU	Luleå University of Technology
SSI	Soil-Structure interaction
TDOK	Swedish Road Administration document
TK Geo	Swedish Road Administration's demands for geotechnical structures
TRVFS	Swedish Road Administration's regulations
TRVK Bro	Swedish Road Administration's demands for bridge design
TRVR Bro	Swedish Road Administration's advice for bridge design

CONTENTS

1. INTRODUCTION

1.1. Background

A bridge is a structure designed to carry the users from point A to point B crossing an obstacle, thus making it very important to know about the loads acting on the bridge as well as the structural response to those loads. There are many different types of bridges which fulfils different requirements, e.g. suspension bridges, cable stayed bridges and arch stayed bridges. These bridges are in general used for long spans and long distances. For shorter spans, frame bridges or beam bridges are usually used (Sundquist, 2009). These bridges can be made either with or without joints transferring movements and forces that acts on the bridge structure. One major problem regarding bridges with joints are the fact that the joints must not be exposed to water or dirt in order to function sufficiently. This will give high maintenance costs, something that will be avoided using jointless bridges, where instead moments are introduced to the rigid connections.

To categorise jointless bridges, the expressions integral bridges or integrated abutment bridges are often used. Examples of integrated bridges are slab bridges, frame bridges, beam bridges or semi-integrated bridges. In most of the integral bridges, the abutments are used to lead both horizontal and vertical forces into the ground. A foundation of either spread foundations or piles are then used. A semi-integrated abutment bridge is distinguished by backwalls placed at the bridge ends taking up the horizontal forces. The bridge superstructure is then connected to adjacent piles through sliding bearings to handle the vertical forces.

Integral bridges are mostly used in Sweden, Finland, England, the United States of America and Canada, with slightly different appearances. In England and North America fully integrated bridges are commonly used, which are characterised by its jointless construction and integrated backwalls supported by piles. In Sweden and to some extent also Finland, it is more common to use semi-integrated bridges, or frame bridges with spread foundations (Kerokoski, 2006).

The horizontal forces, e.g. braking forces or restraining forces induced by temperature movements, generates an increase of earth pressure behind the abutment. Mutually for both the integrated and semi-integrated abutment bridge is the interaction with the surrounding soil, inappropriate capacity can lead to failure in the soil or inadequate support of the bridge foundation. Another failure mode can be for example contraction of the structure leading to settlements.

Soil-structure interaction, SSI, is a complex phenomenon and results from analysis concerning SSI may vary depending on the theory used and ground conditions. For example, when analysing a jointless slab bridge in a finite element-program (FE-program), the soil has to be modelled in an adequate way to be able to capture the section forces, thus giving reasonable

dimensions of the backwalls, or frame legs, interacting with the soil. The boundary between the soil and the bridge can be modelled as springs, either linear or nonlinear, with the same stiffness as the soil, or as a solid mass. Methods for calculating by hand also exist, and they are restricted by the Eurocode and the demands from the Swedish Road Administration. One of the biggest problems with the computer models is the fact that the boundary conditions concerning the soil stiffness are very complex and hard to find. One way to verify the model is to perform measurements of actual structures, measuring for example earth pressures, temperatures, and displacements. The original FE model is then updated to correspond to the real behaviour of the structure (Karoumi, et al., 2007).

In this dissertation, a method for FE modelling of the deformations and section forces in a fully integrated abutment bridge and a semi-integrated abutment bridge with backwalls is studied, and also the extent of the soil-structure interaction. A case study of an actual bridge in Finland is therefore performed, and the idea of modelling the surface between the soil and the structure as linear springs are going to be investigated. The results from the FE model shall be compared to both the calculations from the codes and measured data, which earlier has been performed on the bridge from the case study.

Chapters 2, 3 and 4 is part of the literature review performed to gather basic knowledge about the topic of the dissertation concerning jointless bridge types, soil-structure interaction and general loads on bridges.

Chapter 5 presents the bridges of the case study, as well as the measurement data used to verify and update the model.

Chapter 6 presents the calculations of the loads acting on the bridge. These loads are later inserted in the FE model. Also bending moments at the boundary between backwall and bridge slab is calculated through a simple load case.

Chapter 7 explains how the models are defined, and how it is set up and what characterises the models. Then the iteration of the soil stiffness is performed in chapter 8.

Chapter 9 presents the results and a discussion from the analysis as well as comparison of the moments calculated by hand and the ones fetched from the FE model and chapter 10 summarises the conclusions and presents ideas for further research.

1.2. Aims and scope

The main aim of the dissertation is to find FE models with good agreement to the real response of jointless bridges subjected to horizontal forces, through a method that combines an initial model calculated from the standards provided by the Swedish Road Administration and measured data of a real bridge. To do this, firstly a literature review is made with the aim of providing more knowledge of the soil-structure interaction and case of horizontal forces on bridges, and secondly a case study of a Finnish bridge is performed ending up in a computer model.

The following issues are going to be answered:

- Is the method of modelling the surface between the soil and structure as linear springs applicable?
- Does the stiffness calculated from measurement data correspond to the stiffness giving the correct displacement in the FE model?
- How comparable are the bending moments calculated from a simple load case of a cantilevering beam and the loads given by the Swedish codes and regulations, and the bending moment given by the FE model?

The models shall provide a verification of the calculations done with respect to the codes, comparing the accuracy. Also it shall give a better understanding for the important parameters that influences the design work and how the soil-structure interaction works for jointless bridges.

1.3. Method

A literature study is made in order to examine existing literature on the subject of integral bridges, loads on bridges, earth pressure theory and soil-structure interaction, including journal articles and prior theses. The conventional codes and regulations are used to calculate the section forces. The model is then analysed with the computer program Brigade/Plus and modified against the measured data to gain an accurate FE-model.

The method used in the project can be related to a common method called Structural Parameter Identification. Principally, a structural model (i.e. a FE model) will give loads and responses as well as the section forces, which can be used when designing the structure. Often an optimization is done regarding the actual response, taking into account measurements from real structures. The two results, the structural model and the measurements, is then combined to capture the real response in an FE-model (Karoumi, et al., 2007).

An update of the structural model with respect to the measured data requires good understanding of sensitive parameters and the structural modes. The method of Structural Parameter Identification is briefly described below, but the interested reader is referred to *Modern mät- och övervakningsteknik för bedömning av befintliga broar*, a report by four of the leading universities in Sweden; KTH, LTU, CTH and LTH (Karoumi, et al., 2007).

Methodology of Structural Parameter Identification:

- Set up of structural model
- Uncertainties and sensitivities with the model
- Estimation of critical parameters
- Eventual improvement of model
- Perform measurements and collect data
- Perform Structural Parameter Identification
- Update the initial structural model

The method used in this dissertation is based on Structural Parameter Identification. An initial model is set up with regards to the parameters of the bridge, as well as the actions acting on the bridge. Then the measurements of the actual structure is preformed and the data collected from Tampere University of Technology is evaluated and used to update the initial model.

The methodology of the dissertation is summarised as:

- Deriving of soil stiffness
- Development of the loads acting on the bridge
- Set up of initial model in Brigade/Plus
- Evaluation of the measurement data and development of the new soil stiffness
- Updating of the initial model with regards to the new soil stiffness
- Evaluation of the results

1.4. Limitations

The literature review is focused mainly on the soil-structure interaction, thus only giving a general introduction and presentation of the bridge type used in the dissertation as well as basic theory regarding loads on bridges. The earth pressure theory is explained to give a better understanding about the underlying problems to the soil-structure interaction.

Two types of jointless bridges are going to be studied, the fully integrated abutment bridge and the semi-integrated abutment bridge. The soil is going to be modelled as linear springs, having increasing stiffness with increasing depth in the soil. The stiffness are controlled, and limited, by the displacement of the backwall and the earth pressure induced behind it.

In the analysis, only the horizontal forces and movements are considered, i.e. temperature movements, braking forces, the lateral at rest earth pressure and surcharge load. These loads are used to calculate the section forces in the top of the backwall, and the section forces are compared to those given by Brigade/Plus.

2. BRIDGE TYPES

One of the most common bridge types in Sweden is the slab bridge (Karlsson & Welinder, 2011). The slab bridge can be constructed either with or without joints, but because the focus of this dissertation is bridge without joints, these are the only ones considered further. Slab bridges are mostly built for shorter spans in the range of 15-25 m with reinforced concrete, and up to 35 m if prestressed concrete is used (Sundquist, 2009). Slab bridges are used in many cases because of its many advantages any few restrictions, for example it is easy to construct, and can be economically beneficial, in comparison to other types of bridges when short bridge spans are needed (Sundquist, 2009). Wendner et al. (2011) explain another advantage with the slab bridge. No joints are used, which means that the ride becomes smoother due to the continuous superstructure. Also, it is beneficial to use a slab bridge when the height of the structure needs to be small (Swedish Road Administration, 1996).

The beam bridge is the simplest type of bridge with regard to the load bearing. They can be made longer than slab bridges, up to 200 m, and are more suitable for longer spans than slab bridges due to less material use, and thus less self-weight (Sundquist, 2009). In some cases, the bridge slab is a combination of both beams and slab, i.e. a slab-and-beam bridge, and in some cases the beams can be made of steel and the slab of concrete, i.e. a composite bridge. Two typical executions of cross sections is shown in figure 2.1.

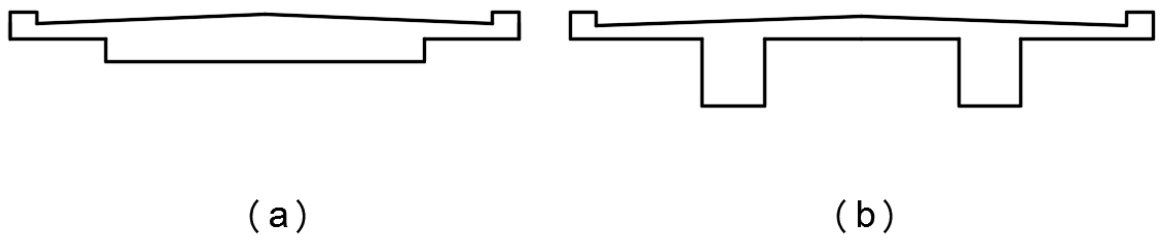

Figure 2.1. Typical executions of cross sections of (a) a slab bridge and (b) a slab-and-beam bridge.

2.1. Jointless bridges

Slab or beam bridges can be made without joints and bearings, a feature that makes them more cost effective than other types, since it reduces the required maintenance costs and increases the bridge durability (Pétursson, 2000). Reinforcement and other components are protected against water, and thus corrosion etc., because of the compact composition. On the down side, no joints means moment stiff connections and risk for high restraint forces. The longer the bridge is, the larger the restraint forces might become, meaning that long bridges have difficulties taking up the restraint forces (Sundquist, 2009). This adds to the argument

that jointless bridges are more suitable for shorter spans. Also the height of the backwalls affects the magnitude of the amount of restraint forces in the structure, higher (deeper) backwall gives lower restraint forces (Sundquist, 2009).

The generic term of the jointless bridges is often integral bridges, or integral abutment bridges, because the bridge abutment and foundation is integrated in the bridge superstructure without the use of any joints or bearings. Integral bridges can be made longer than the typical slab bridge, with spans up to 100 m (Lock, 2002).

The main focus in the dissertation is to study jointless bridges with backwalls. A backwall is a structural element found on the end of the bridge, with a purpose of protecting the end support of the bridge from lateral earth pressure, due to temperature movements and braking forces (Swedish Road Administration, 1996). In this dissertation the structural component interacting with the soil will be denoted 'backwall'. In other literature, it can be named e.g. 'end-screen' or 'breast wall'. Different abutments of jointless bridges are found in figure 2.2. Most of the backwall bridge types are slab bridges and beam bridges, which includes frame bridges ((a) and (b)), fully-integrated abutment bridges (i.e. integral bridges) ((c) and (d)) and semi-integrated abutment bridges (i.e. bridges with backwalls) ((e) and (f)). The jointless bridge can be used for road traffic, train traffic and pedestrian traffic.

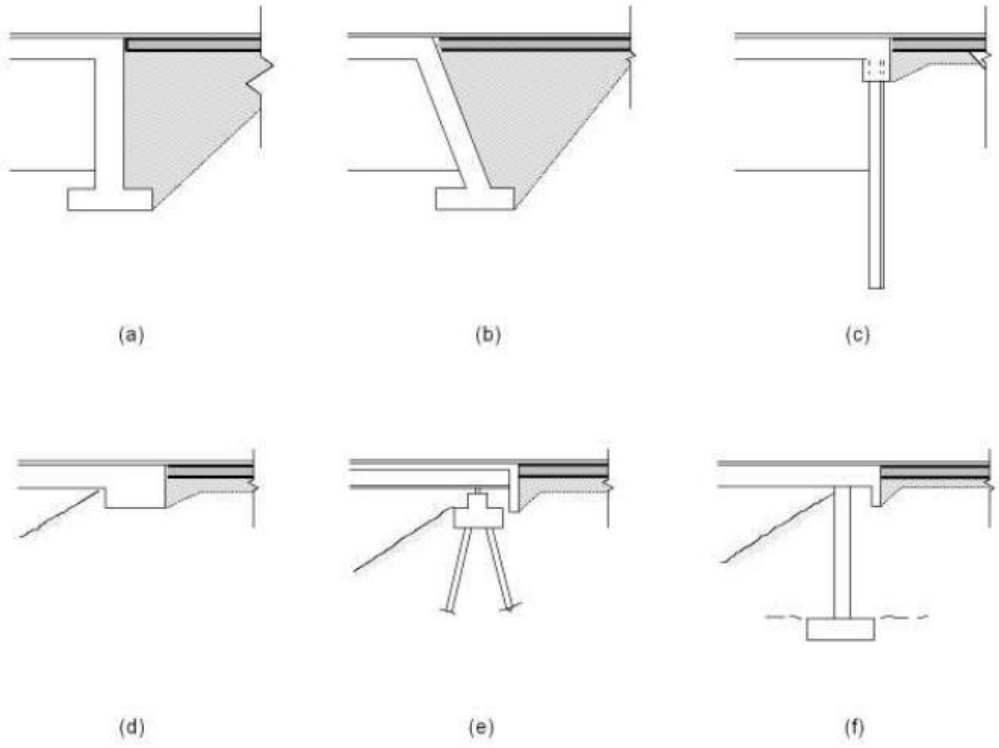

Figure 2.2. Different bridge abutment types, the one studied in this dissertation is type (c) and (e) (Highways Agency, 2003).

The load bearing of a bridge without joints is good due to frame action, i.e. the horiozontal forces are handled by the moments occurring in the frame corners. Also the stiffness is improved, as well as both the internal force distribution and the seismic performance due to frame action (Malerba & Comatia, 2014). The horizontal forces are taken up by the

backwalls, and the vertical forces can be taken up by either the backwalls or adjacent piers, illustrated in figure 2.3, depending on the bridge type (Carlstedt, 2008).

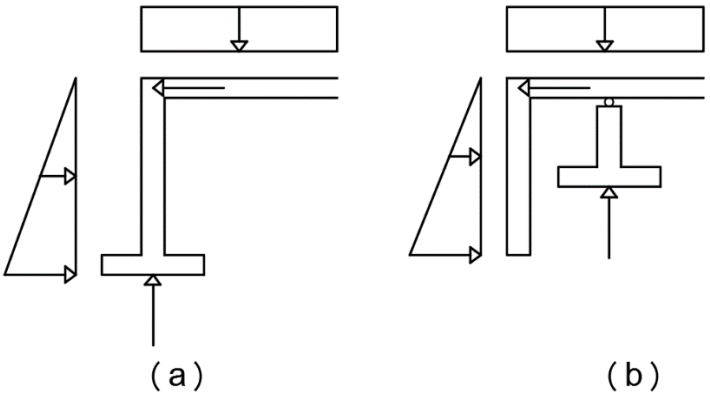

Figure 2.3. Conceptual load bearing of (a) a frame bridge with spread foundation, or a fully integrated bridge with pile foundation, where both horizontal and vertical forces are taken by the frame legs and (b) semi-integrated abutment bridge with backwall where the vertical forces are taken by adjacent piers and the horizontal forces are taken by the backwall.

One disadvantage with the bridge with an integrated backwall is the fact that modelling the soil plays a major role in respect with reinforcement (Carlstedt, 2008). Since the soil-structure interaction is a complex phenomenon, the structures tend to be very heavy and over dimensioned, and one of the reasons for this is that the calculated maximum passive earth pressure is not reached (Zhang, et al., 1998). This subject will be discussed later in the dissertation.

2.1.1. Fully integrated abutment bridges

The fully integrated bridge is characterized by its effectiveness of load bearing due to frame action, and can be carried out both as a beam bridge or a slab bridge. The fully integrated bridge is one of the simplest bridges without bearings, and can be paired with a frame bridge, but with pile foundation. The bridge deck is load bearing and both the vertical and horizontal forces are taken up by the frame legs, i.e. the backwalls (Carlstedt, 2008). The frame legs also needs to be able to take the moments and restraining forces developed in the bridge, the amount of reinforcement controls the span ratio and bridges that are prestressed can be made longer (Carlstedt, 2008).

Due to the large amount of concrete needed when building a jointless bridge, the slab is recommended by the Swedish Road Administration to be constructed as a hollow-core slab (Swedish Road Administration, 1996). The holes will reduce the dead weight, otherwise the frame bridges tends to be very heavy, which leads to higher quantity of reinforcement.

2.1.2. Bridges with backwalls

Similar to the fully integrated bridge, the bridge with backwall (or semi-integrated abutment bridge), takes up the horizontal forces in the backwalls, due to increased earth pressure in the backfill soil against the backwall (Swedish Road Administration, 1996). However the vertical forces are taken by the adjacent piers situated in front of the backwalls (Carlstedt, 2008). One advantage with this performance is that the foundation work can be executed in dry conditions, another is that the foundation is easier to inspect (Swedish Road Administration, 1996). It is notable that the semi-integrated abutment consists of an adjacent pier, connected to the superstructure with a bearing, and a backwall. According to Sundquist (2009), though it is a disadvantage that a bearing is used, it can be placed so that it is protected by the backwall.

The main task of the backwall is to absorb the forces from braking vehicles and temperature changes (i.e. horizontal forces) (Carlstedt, 2008). Then it can be beneficial to use friction soil, e.g. blasted rock, as counter filling because of its good characteristics regarding deformations and settlements. If the foundation is placed on rock or soil with less capacity, e.g. clay, use of higher backwalls are needed, and in case of good soil, e.g. firm friction soil a lower backwall can be used (Swedish Road Administration, 1996).

3. SOIL-STRUCTURE INTERACTION

The bridge interacts with the soil at the boundary between the two elements. The backwall movement type and the stresses induced behind the backwall are strongly dependent, as well as the composure of the backfill soil. The backfill soil is the soil that is put in behind the abutment after an excavation of the original soil. It is the passive earth pressure, due to the fact that the structure presses against the soil (backfill), which is of interest (Bayoglu Flener, 2004). Although the standards only suggest that the bridges are to be designed for the at rest earth pressure. There are three stages of earth pressure (Sällfors, 2009):

- At rest earth pressure is when the soil and structure is in equilibrium
- Active earth pressure is when the soil stress acting on a structure contributes to a failure
- Passive earth pressure is when the structure moves against the soil, causing stresses

Parameters that affects the stresses that occur in the structure are the length of the bridge and the height (depth) of the backwall. Also, the skew of the bridge can cause difficulties. A skewed bridge means that the abutment line is not perpendicular to the center line of the bridge roadway (Sundquist, 2009). Hassiotis and Xiong (2007) describes that the skew will initiate rotation in the bridge superstructure due to the earth pressure. According to White et al. (2010) the maximum skew is 30° in many countries. In Sweden though, there are no maximum allowed skew.

Cyclic loading can occur, i.e. due to changes in temperature and due to traffic. According to Bloodwoth et al. (2012) sand is more sensitive with respect to stress increase due to cyclic loading. The traffic load will cause a displacement in the backwall, and thus a passive earth pressure in the backfill soil. Backwall movement will compact the soil more and more for each time. This procedure will eventually cause the pressure to increase towards the passive earth pressure (Bayoglu Flener, 2004).

Similarly the temperature movement in the structure causes deformations in the backwall. According to Fartaria (2012) the worst cases are the summer days and the winter nights and likewise Carlstedt (2008) describes in her dissertation that the biggest issue is the temperature difference between summer and winter. This is because the largest temperature span, i.e. the largest temperature difference, is between the two extreme values (highest temperature in the summer and lowest temperature in the winter). The difference between the temperature movement and the traffic-induced movement is their duration. The temperature changes spans over a longer time period and induces a larger magnitude in movement, thus making it a more crucial factor (Carlstedt, 2008).

Cyclic loading can also be the origin for settlements of the abutment. The risk for settlements is highest during the winter when the bridge is decreasing in length (Fartaria, 2012). The

length decrease will lead to a decrease of the earth pressure, thus causing settlements. Also, White et al. (2010) relates the risk of settlements to the foundation type. A spread foundation is better rather than a pile foundation. The conceptual difference between the two foundations is illustrated in figure 3.1. Because the spread foundation have a larger "footprint" the load is distributed and reduced, thus decreasing the settlements.

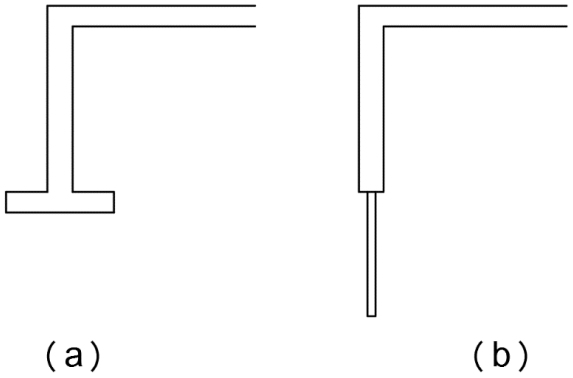

Figure 3.1. Conceptual figure showing the execution of (a) a spread foundation and (b) a pile foundation.

As stated above, the stresses induced in the backfill soil is depending on the displacement of the backwall. The displacement mode of the backwall depends on both the stiffness of the superstructure and the stiffness of the backfill soil (Fartaria, 2012). The mode of the backwall is usually a mix between rotation and translation (White, et al., 2010). Zhang et al. (1998) explanied some examples of wall movements and corresponding stress distributions, and how the earth pressure coefficient changes with the displacement mode of the backwall. For example if the backwall rotates around a point somewhere in the middle of the wall, one part of the wall will be subjected to passive earth pressure, the rotation point will be subjected to at rest pressure and the other part will be subjected to active earth pressure. Rotation about the bottom of the wall will result in active or passive earth pressure, depending on the direction of the rotation, and rest pressure in the rotation point (the base). Some examples of corresponding earth pressures and wall movements are shown in figure 3.2.

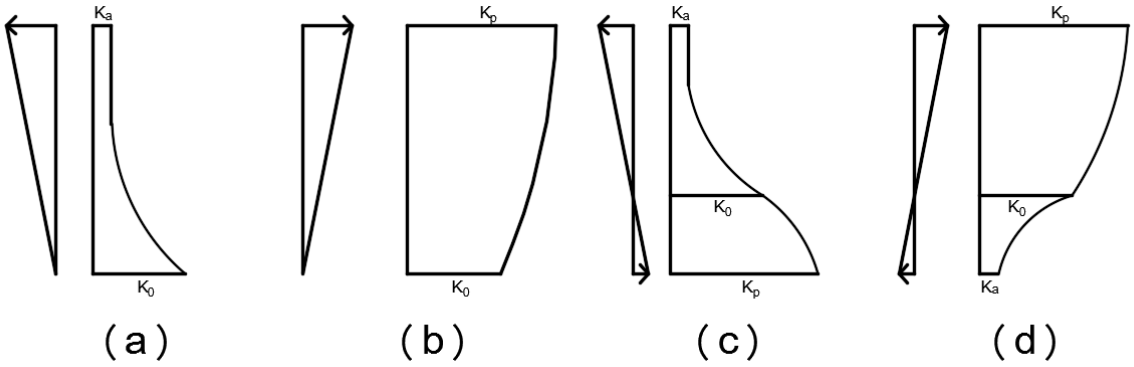

Figure 3.2. Different backwall displacement modes and the corresponding change of earth pressure coefficient, in all figures displacement to the left means active earth pressure and displacement to the right means passive earth pressure.

3.1. Backfill soil

In Sweden, the backfill soil is usually composed with cohesion-less, well-compacted, granular soil (White, et al., 2010). The parameters of the soil are well known, and described in the codes and regulations for each country. According to White, et al. (2010), in the United States the engineer sometimes uses loose sand, and in other counties there are no requirements for the backfill. In Sweden the characteristics is stated in TK Geo (Swedish Road Administration, 2011a).

When constructing the bridge abutments and backwall, the backfill is placed in layers. Each layer has to be compacted before the next is placed (Olmo Segovia, 2006). White et al. (2010) is highlighting the importance of distributing the backfill soil evenly on both sides of the bridge. This is important because it decreases the moments that otherwise would have occurred.

There are different executions that will decrease the lateral earth pressure against the backwall. For example an elastic material, e.g. a geoplate, on the border between backwall and soil will help to ease the pressure (Swedish Road Administration, 1996). Also, the soil can be reinforced to withstand a higher pressure. Wendner et al. (2011) explains the use of geotextiles which will reduce the risk for settlements.

3.2. Problematics regarding lateral earth pressure theory

There are some theories suggesting that failure can occur even if the passive and active earth pressure in the soil is not reached when a structure is loaded. The concern also regards whether the theories used are sufficient enough, because they assume full active or passive earth pressure (Zhang, et al., 1998). If failure occur before the designed earth pressure is achieved, it will cause failure in the soil when the structure is loaded with a much smaller load than expected. Some authors also means that structures are designed with underestimated earth pressures. Further, the common design methods as Coulomb or Rankine theory are reasonable for a plane failure surface, but mostly the failure surface is of a circular shape (Hassiotis & Xiong, 2007). According to Zhang et al. (1998), the displacement of the backwall gives rise to stresses in between the full passive or the full active earth pressure. This is handled in the Swedish standards by calculating the earth pressure in a specific way depending on the displacement found by the load case (Swedish Road Administration, 2011b).

Salman et al. (2010) describes the high dependence between the displacement of a retaining wall and the stresses induced in the soil. It should be noted that a retaining wall and a bridge backwall behaves similar. Vertical deformation of the backwall can occur in different shapes as illustrated in figure 3.3. For example the deformation can take place in the base of the wall, in a point somewhere on the wall or by bending of the wall (Zhang, et al., 1998).

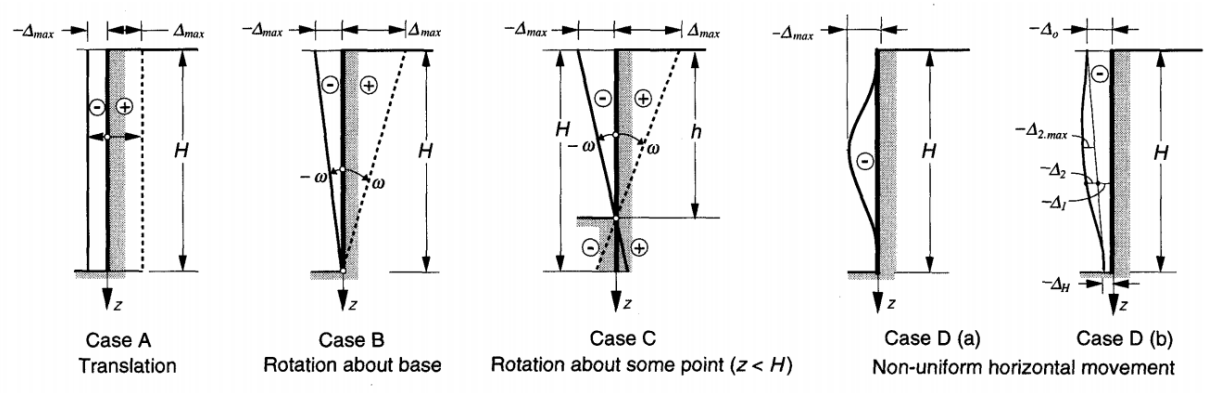

Figure 3.3. Different modes of deformation of the backwall (Zhang, et al., 1998).

The common theories of lateral earth pressure (e.g. Coulomb) are most compatible with rotation about the bottom of the wall (case B in figure 3.3) (Salman, et al., 2010). Though, according to Hassiotis and Xiong (2007) the wall displacement due to lateral earth pressure is a mixture of both translation and rotation, where the rotation is the dominant part. The boundary conditions are the main influence of the displacement mode, e.g. if the abutment is a backwall only taking horizontal forces (i.e. semi-integrated) or if the backwall takes both the vertical and horizontal forces (i.e. fully integrated).

Zhang et al. (1998) states that if ϕ' is constant with the depth, the soil behaves plastically everywhere, and the Mohr-Coulomb criteria applies. If a material behaves plastic, the deformations will sustain even after it is unloaded. Further, most of the time one assumes that ϕ' is constant, but this is an idealization and not good for values between the extreme values. In contradiction, Bloodworth et al. (2012) highlights that the at rest earth pressure will increase significantly after just 300 load cycles and will continue to rise, approaching passive earth pressure.

Rajeev et al. (2014) performed enquiries of the earth pressure theories of Coulomb and Rankine, and stated that Coulomb gives higher values of the passive earth pressure coefficient, and that the Coulomb and Rankine theories function best in the middle and lower parts of the wall. In the upper parts of the wall they tended to overestimate passive earth pressure. This corresponds to the investigations made by Hassiotis and Xiong (2007), arguing that the theories will overestimate the passive earth pressure. The biggest difference between the two methods is that in Coulombs theory, the wall friction angle is taken into consideration (Zhang, et al., 1998).

Investigations made by the British Road Administration and presented in the British code BA42/96 suggests an alternative method of calculating the passive earth pressure coefficient (Rajeev, et al., 2014). This method takes into account both the passive and the at rest pressure coefficient, making it more alike the arguments stated in this chapter. The formula adapted in the code follows from several field experiments. Further, Rajeev et al. (2014) describes that the earth pressure in the lower parts of the wall reduces linearly down to the active earth pressure.

4. GENERAL LOADS ON BRIDGES

There can be many different loads on a bridge, which can arise from changes in temperature, from the traffic that operates the bridge, or from the characteristics of the material, i.e. self-weight or long-term deformations. It is important to know the structural behaviour, and the stresses and strains that can occur due to loading of a bridge, hence it becomes necessary to investigate the origin of the behaviour, i.e. the loads. In this chapter, the main loads that can act on a bridge are presented.

Depending on what material is used, the self-weight of the structure will vary as a result of different densities for different materials. Generally, concrete is a relatively heavy material, thus generating high self-weight. Further types of material dependent load effects for concrete can be for example creep and shrinkage (Burström, 2007). Another issue that should be taken into consideration is the effects of wet concrete when constructing the bridge, when the structure cannot carry its own weight, and the self-weight of the concrete must be taken care of by for example propping the structure (Sundquist, 2009).

Some stresses and strains in bridges originates from the restraining that occurs when the bridge is obstructed to move. This feature will be more perceptible for a bridge without bearings. Loads that can affect a bridge, but are not covered in the dissertation, are e.g. wind, snow and accidental loads, such as explosions, collisions and progressive failures.

4.1. Traffic loads

Traffic loads are movable loads which occur in a random nature, depending on the amount and type of traffic, number of lanes and speed limit. This means that there are large uncertainties regarding traffic loads, and the bridges are usually designed for maximum values (Getachew, 2003). Cars can for example drive in many different lanes, and in many different combinations along the bridge. Other traffic loads can be for example trains and pedestrians, which however are not being considered in the dissertation. Traffic can both cause vertical forces, due to the self-weight of the vehicles, and horizontal forces, due to the braking of the vehicles. Fatigue phenomena occur due to repeated loading and unloading by traffic, and are increased by increasing axle load, braking and acceleration (James, 2003). Rylander (2006) also describes that the traffic loads can have a dynamic effect which is affected by the velocity of the vehicle as well as the weight.

The horizontal component of the traffic load is the braking load, which is a short duration load acting on the upper side of the bridge superstructure. Another load caused by traffic is the surcharge load. The surcharge load originates from e.g. a vehicle standing on the side of the

bridge. This will cause a lateral earth pressure on the adjacent bridge backwall, and a reaction pressure on the other side, see figure 4.1.

Figure 4.1. The priciple of surcharge load, the frame legs, i.e. backwalls, are loaded by a lateral earth pressure.

4.2. Temperature loads

Temperature loads affect bridges due to stress changes, for example when the concrete is heated up, it expands, and when it cools down it contracts again (Burström, 2007). According to Fartaria (2012) the movement mainly happens in the horizontal direction. Reasons to variances in temperature can be for example the radiation from the sun, the wind, and material behaviour such as thermal inertia. Concrete is a material with a relatively low heat conduction capacity, meaning that the heat transfer inside the material is low, making it more sensitive for thermal variations because large differences in temperature will arise within the structure (Larsson, 2012). Further, Larsson (2012) explains that the side of the structure facing south will be more exposed to the sun witch will give a higher temperature of the material in these sections. The lower side of the structure will be cooler than the upper side when the upper side is heated, resulting in expansion in the upper side, and contraction in the lower side (Larsson & Svensson, 2013). This is because of the material heat tardiness, and the differences in temperature within the material.

The stresses and strains caused by the thermal actions are initiated by the restraining of the structure, i.e. because the structure is obstructed to move. Restraining forces increase with increasing dimensions, and is closely connected to the moment of inertia, and thus stiffness, of the structure (Larsson, 2012).

4.3. Earth pressure

Soil can be divided into two main groups, cohesion soil, e.g. clay, and friction soil, e.g. sand. The friction soil is characterized by the internal friction angle ϕ', which describes the angle of the line for the shear stress in the Mohr-Coulomb's circle, and also describes the limit angle of

the surface of the material. The stress history of the soil is described by the consolidation, i.e. how much it is compacted. This matters with respect to the risk of settlements (Sällfors, 2009). The stresses that occur in the soil are characterized by the principal stresses σ_1, σ_2 and σ_3. They can be found by performing tests on the soil, e.g. a triaxial loading test, along with the shear stress τ_{xy} (Zhang, et al., 1998).

The passive and active earth pressure will give rise to different failures modes not only in the backwall, but also in the soil. The failure mode is partly characterised by the internal friction angle, and the angle is illustrated in figure 4.2. By comparing the earth pressure coefficients, the passive earth pressure is approximately 25 times larger than the active earth pressure.

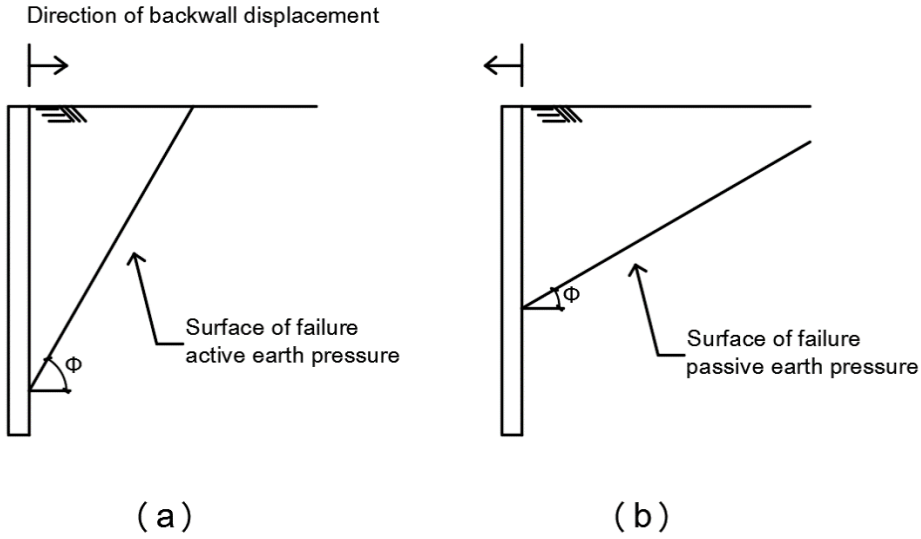

Figure 4.2. The internal friction angle both according to (a) active earth pressure and (b) passive earth pressure.

Changes in earth pressure behind a backwall occur due to horizontal loading of the bridge superstructure, which are transferred to the backwalls. For example temperature changes of the bridge can induce a passive earth pressure if the bridge expands, and an active earth pressure if the bridge contracts. There can also be an increase in earth pressure over time, e.g. by cyclic changes of the temperature due to the compaction of the soil (Bloodworth, et al., 2012). Also the stresses are largely dependent on the deformation shape of the backwall. The backwall can either translate or rotate and the rotation can arise both in the base, middle or top of the wall (Salman, et al., 2010).

4.3.1. Lateral earth pressure

The vertical loads, both external loads and the weight of the soil, spreads down in the ground. The self-weight of the soil magnifies with increasing depth and the stresses are calculated by multiplying the weight of the soil with the depth. To transform the vertical loads, denoted σ_1, into horizontal components, i.e. σ_2 and σ_3, the stress is multiplied with the earth pressure coefficient K. The coefficient K_0 represent the earth pressure coefficient at rest, K_a the earth

pressure coefficient for active earth pressure and K_p is the coefficient for the passive earth pressure (Zhang, et al., 1998).

The earth pressure that occurs horizontally due to vertical loading from external loads and self-weight of the soil can be calculated as (Zhang, et al., 1998):

$$p = (\gamma z + q)K \tag{4.1}$$

where:

$q =$ external load
$\gamma =$ unit weight of soil
$z =$ depth in soil

For a leaning surface the external load q is divided by $\cos(\alpha)$. The earth pressure coefficient K is either K_0, K_a or K_p and defined by (Zhang, et al., 1998):

$$K_0 = 1 - \sin(\phi')\ ^{1} \tag{4.2}$$

$$K_a = \tan^2\left(45° - \frac{\phi'}{2}\right) \tag{4.3}$$

$$K_p = \tan^2\left(45° + \frac{\phi'}{2}\right) \tag{4.4}$$

where:

$\phi' =$ internal friction angle

Vertical earth pressure is greatly affected by the vertical deformation in the soil. This means that for different types of loading and different boundary conditions, different deformation will occur of the backwall. This fact will give different types of stress distributions in the soil (Zhang, et al., 1998). It should be noted though, that for most cases of general soils the earth pressure coefficients are already calculated and can be taken from tables in the standards.

[1] This formula is valid for friction soil and silty soil (Swedish Road Administration, 2011a)

5. CASE STUDY

A case study is performed, investigating the soil-structure interaction of jointless bridges. The studied bridges are analysed by means of the deformations and earth pressures behind the backwall due to horizontal loading. The case study is going to include two bridges of equal geometrical appearance, but different load bearing system, i.e. one fully integrated bridge and one semi-integrated bridge. Because the FE-models needs to be modified against measurement data, at least one of the bridges needs to be a bridge where measurements have been made, and serve as a reference object. For this purpose, the Haavistonjoki Bridge is chosen as the reference object. On this fully integrated bridge, measurements were performed during the years 2003-2008 (Kerokoski, 2006). The second bridge will be a fictitious bridge, with the same dimensions as the Haavistonjoki Bridge, but the structural system as a semi-integrated bridge.

5.1. Haavistonjoki Bridge

The primary bridge, which will serve as the reference bridge, is the Haavistonjoki Bridge located north east of Tampere in Finland. It is a road bridge, and functions as a highway bridge crossing the Haavistonjoki River. The bridge is a 3-span, fully integrated, jointless slab bridge (Laaksonen, 2011). The bridge have four columns and two backwalls, founded on 8 piles of diameter $0{,}711\,m$. The bridge is $11{,}5\,m$ wide and $56\,m$ long, with span length $15{,}5\,m$, $19\,m$ and $15{,}5\,m$ respectively, see figure 5.1 for full information about the dimensions.

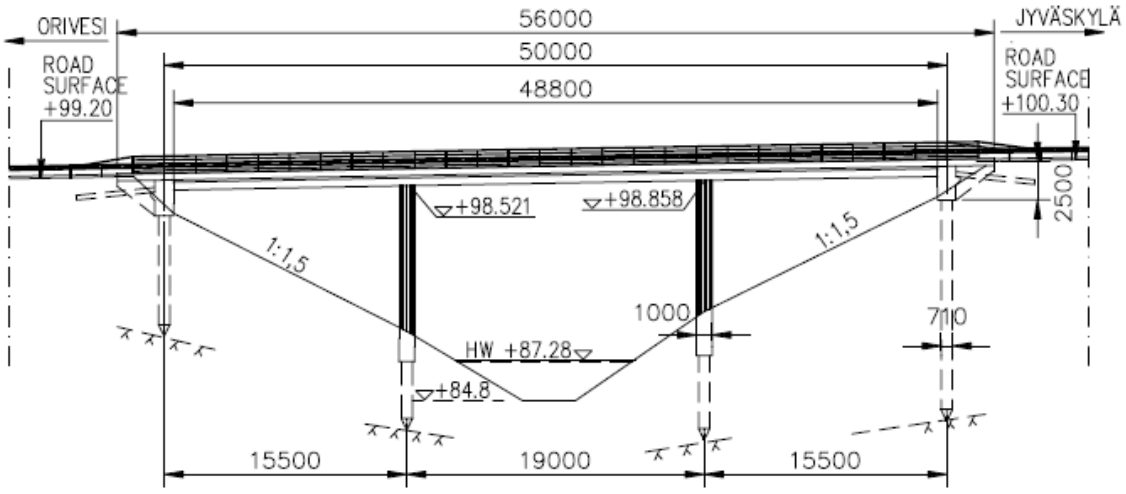

Figure 5.1. Elevation of Haavistonjoki Bridge, containing full information about measures (Kerokoski, 2006).

The bridge has no skew and the backwalls supports the bridge both in the vertical and the horizontal direction. Wing walls are connected to the backwalls, and the bridge slab is a reinforced concrete section with varying thickness in the transverse direction, illustrated in figure 5.2.

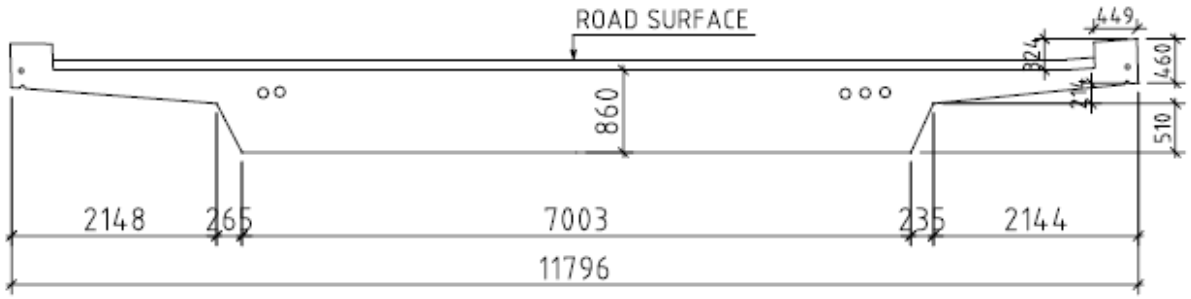

Figure 5.2. Cross section of Haavistonjoki Bridge (Kerokoski, 2006).

The geometry of the backwall is width $11{,}5\ m$, height $2{,}5\ m$ and thickness $1{,}2\ m$, shown in figure 5.3.

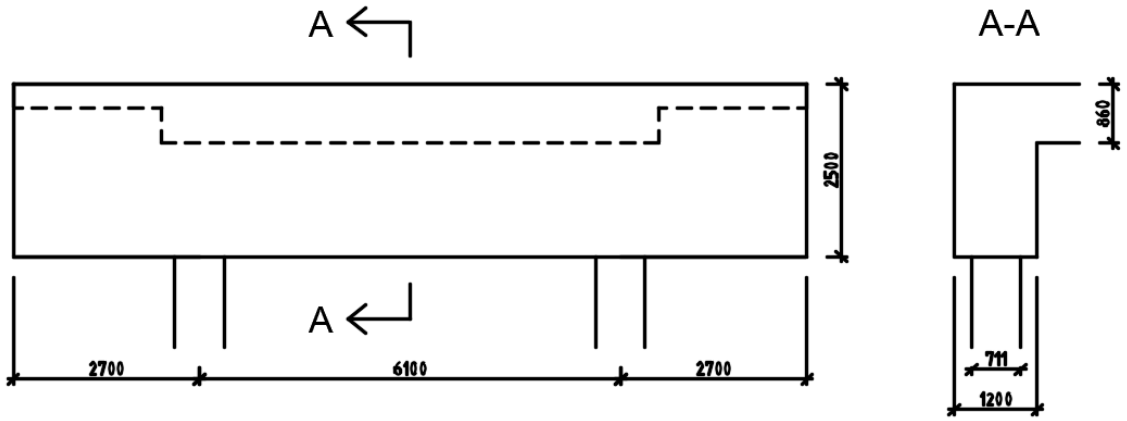

Figure 5.3. Cross section and section of the backwall, also showing the location of the piles.

5.2. Semi-integrated bridge

The second bridge is a fictive bridge with basically the same measures as Haavistonjoki Bridge regarding bridge length, bridge width and backwall height. Also the thickness of the bridge slab and backwalls are the same as for the reference bridge. The difference is the structural system, the fictive bridge is a semi-integrated bridge with backwalls, hence the backwalls will only take the horizontal forces and the vertical forces is handled by intermediate columns. The fictive bridge then consists of a bridge slab, two backwalls and eight columns, the elevation of the fictive bridge is shown in figure 5.4.

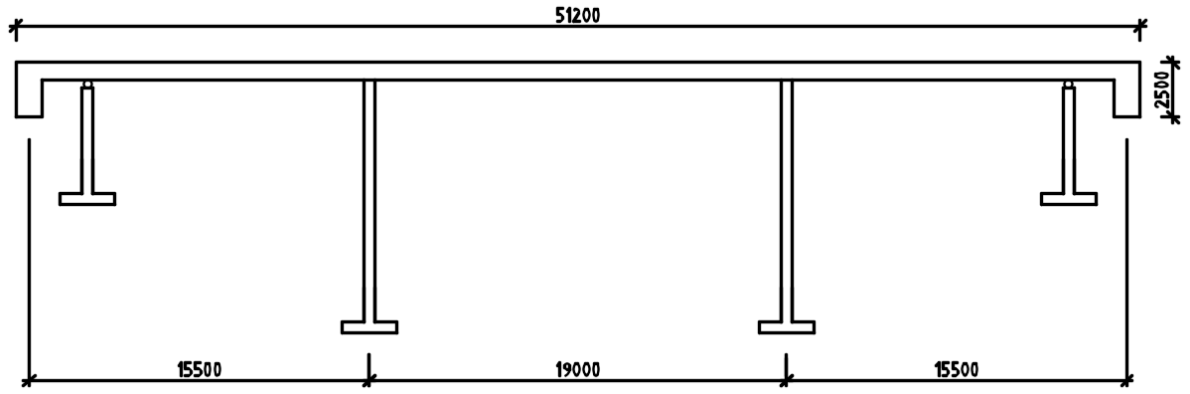

Figure 5.4. Elevation of the semi-integrated bridge, including measures.

5.3. Monitoring of Haavistonjoki Bridge

In total, 191 gauges were placed on the bridge during the construction of the bridge in year 2003, measuring the earth pressures and displacements over a period of 5 years. The measurements were presented in the doctoral thesis of Professor Olli Kerokoski and the doctoral thesis of Professor Anssi Laaksonen at Tampere University of Technology, and for full details of the monitoring procedure, the reader is referred to their works (Kerokoski, 2006; Laaksonen, 2011). The measured data consisted for instance of:

- Earth pressure between backwalls and the surrounding soil at different temperatures of the bridge slab
- Earth pressures between piles and surrounding soil
- Displacements of the backwalls due to a certain earth pressure
- Axial stresses in the piles
- Bridge length change

The used measurement system involved earth pressure cells (EPC), strain gauges, tacheometers, laser distance-meter and temperature gauges.

Also loading tests were performed on the bridge, including a heavy crane and braking test, overrun test and static test. Only the braking test is of interest in this dissertation. The loading test took place in the autumn, when the bridge had started to contract and the backwall displacement where minimum in magnitude (Laaksonen, 2011). Information about the test crane is provided in appendix A (in Finnish).

5.4. Evaluation of the measurement data

The measurement data of interest for the investigations in this dissertation is the earth pressures and displacements monitored for the temperature change corresponding to a long load duration and the braking load corresponding to a short load duration. The results from the measurement of the earth pressures at different temperatures of the bridge slab, as well as the corresponding displacements of the abutment, and the earth pressure and displacement from the heavy crane is presented below. The curves are evaluated with respect of the earth pressure difference over a period of time, and this earth pressure is the force that determines the stiffness of the soil-structure interaction.

The change of temperature will cause the bridge to expand and contract, and an increase or decrease in earth pressure will appear. Professor Olli Kerokoski explains that the period of interest is between 11th of February to the 15th of February 2004 because the largest increase in air temperature occurred during this period. A total of 12 EPCs were placed on the backwalls, with a distribution of 10 on the east backwall (T4) and two on the west backwall (T1) (Kerokoski, 2006). The EPCs were labelled with letters and the placements on the eastern backwall are presented in figure 5.5.

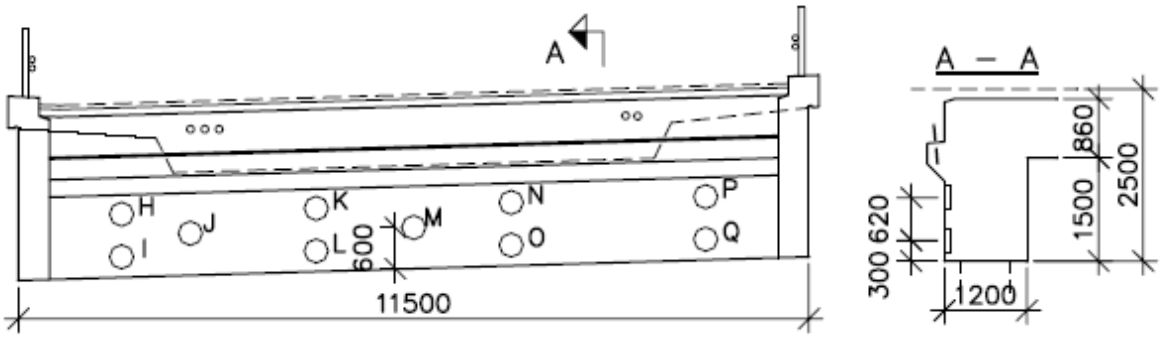

Figure 5.5. Placement of the EPCs on the back surface of the eastern backwall (Kerokoski, 2006).

The measured earth pressures for each point is presented in figure 5.6, note that the cells H-Q is placed on the eastern abutment and V-W is placed on the western abutment. The earth pressure differences for each point is presented in table 5.1.

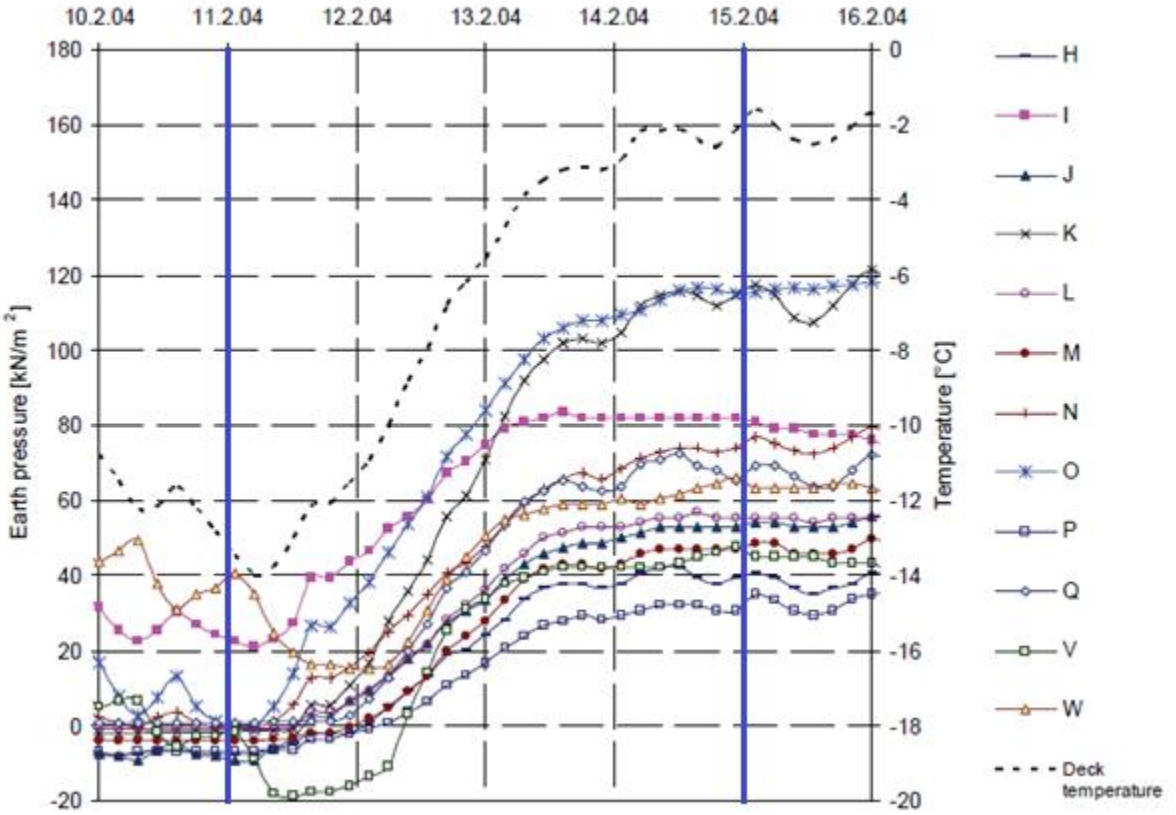

Figure 5.6. Measured earth pressures at specified days, and the corresponding temperature in the bridge slab. The EPCs H-Q is placed on the eastern abutment and the EPCs v-w is placed on the western abutment. The period of interest is shown in the figure (Kerokoski, 2006).

Table 5.1. Earth pressure difference calculated from the measurement data.

Point	**Earth pressure difference** $(\boldsymbol{kPa})$
H	45
I	60
J	65
K	120
L	55
M	55
N	80
O	120
P	40
Q	70
V	70
W	45

The deck temperature at the period of interest varied between $-14\,°C$ and $-2\,°C$, and increased during the period. The earth pressure near the wing walls is significantly lower than the earth pressures in the middle of the backwall. This is because the wing walls provides stiffness to the structure, as well as the embankment soil being less stiff near the edge of the

backwall (Kerokoski, 2006). On account of this, the resulting earth pressure on the backwall due to temperature change is calculated as the mean value of the measured earth pressures from the middle EPCs. This gives the earth pressure $p_{T4} = \frac{120+55+55+80+120}{5} = 86\ kPa$.

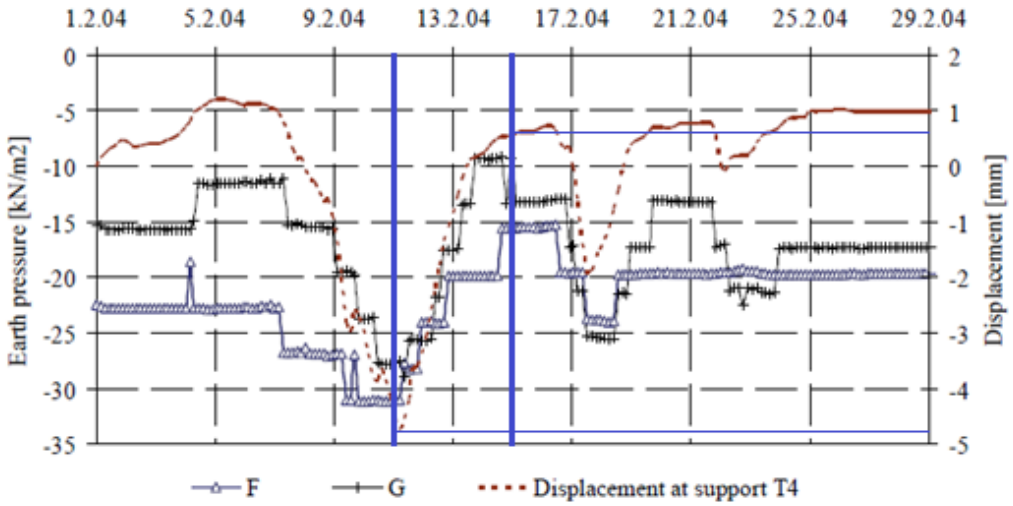

Figure 5.7. The displacement and measured earth pressures of the eastern abutment (T4). The reading of the displacement is shown in the figure (Kerokoski, 2006).

The displacement of the eastern abutment (T4), measured at a depth of $z = 0{,}15\ m$ below the top of the backwall, is shown in figure 5.7, and varies between $\delta_{max} = 0{,}6\ mm$ and $\delta_{min} = -4{,}7\ mm$ during 11th-15th of February. This gives a total displacement of $\delta_{T4} = 0{,}6 - (-4{,}7) = 5{,}3\ mm$.

The displacement of the western abutment (T1) is significantly smaller than the displacement of the eastern. From the thesis by Kerokoski it appears that the resulting displacement of the western abutment (T1) is $\delta_{T1} = 0{,}3\ mm$ (Kerokoski, 2006).

The large variation of earth pressure differences in the gauges seems unlikely, as well as the large difference in backwall displacement between the eastern and western abutment. For the purpose of model updating and comparison of the two bridge types though, this is disregarded and the continuous calculations are performed with this in mind.

The braking test provided diagrams of earth pressure, displacement and the velocity of the crane, presented in figure 5.8.

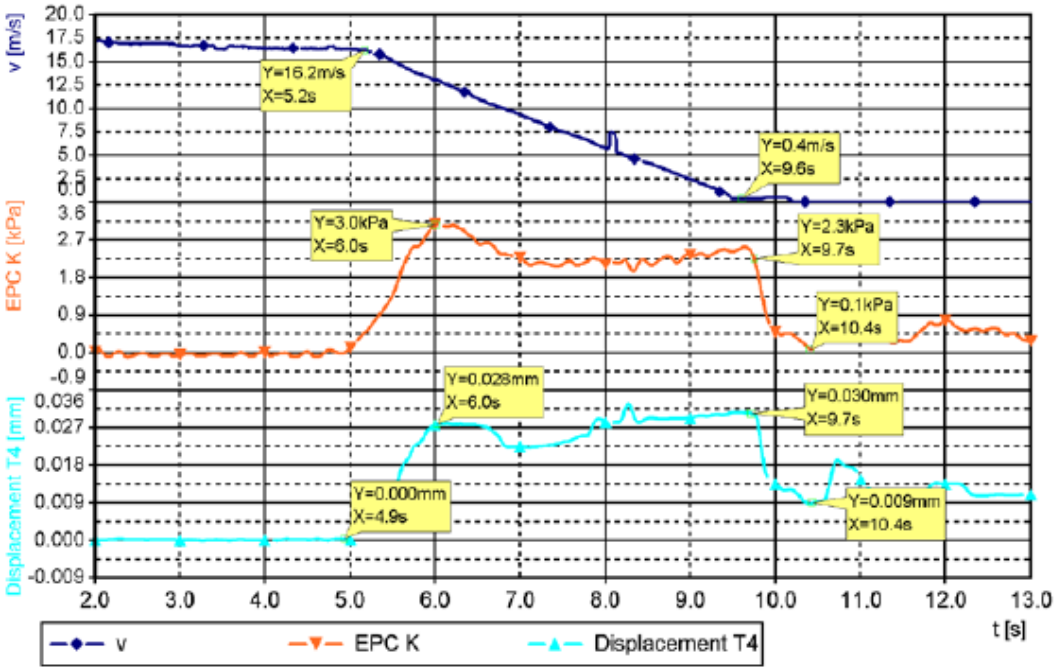

Figure 5.8. The test results from the braking test, the upper curve shows the velocity of the truck, the middle curve shows the measured earth pressure and the lower curve shows the corresponding displacement (Laaksonen, 2011).

The yellow boxes in the figure corresponds to the different states of the braking of the crane. The upper line shows the velocity, $v_0 = 16{,}2\ m/s$ at time $t_0 = 5{,}2\ s$ and $v = 0\ m/s$ at time $t = 9{,}6\ s$. The middle line shows the variation of earth pressure due to the decreasing velocity, starting at $p_0 = 0\ kPa$ at the constantly moving crane and rising to the maximum earth pressure $p_{max} = 3\ kPa$. The pressure is then roughly constant during the time of deceleration of the truck. The lower line shows the displacement taking place in the abutment during the deceleration. The maximum displacement taking place is $\delta = 0{,}03\ mm$.

The braking force from the 60 ton crane acting on the bridge is calculated from the relation between the force and the acceleration, i.e. $F = ma$.

$$a = \frac{\Delta v}{t} = \frac{16{,}2 - 0}{9{,}6 - 5{,}2} = 3{,}68\ m/s^2$$

$$F_{B,crane} = 60 \cdot 3{,}68 = 220{,}8\ kN$$

The earth pressures and corresponding displacements for both abutment T1 and T4 are summarised in table 5.2 below.

Table 5.2. Earth pressure differences calculated from the measured data, and the corresponding displacements.

Load case	**Earth pressure difference (kPa)**	**Abutment displacement (mm)**
Temperature (T4)	86	5,3
Temperature (T1)	57,5	0,3
Braking (T4)	3	0,03

5.4.1. Soil properties based on analysis of the surrounding soil

Field tests and laboratory tests have also been performed on the surrounding soil, determining the properties. The backfill material consists of well-compacted crushed rock with properties presented in table 5.3 (Kerokoski, 2006).

Table 5.3. Backfill soil paramteres determined from field tests.

Parameter	**Value**
Self-weight, γ_{bf}	$20\ kN/m^3$
Internal friction angle, ϕ'_{bf}	42°
Cohesion, c	0

The earth pressure coefficients is calculated from eq.4.2 and eq.4.4.

$$K_0 = 1 - \sin(\phi'_{bf}) = 1 - \sin(42) = 0{,}33$$

$$K_p = \tan^2\left(45 + \frac{\phi'_{bf}}{2}\right) = \tan^2\left(45 + \frac{42}{2}\right) = 5{,}05$$

Under the backfill soil a layer of silt is located, and below the silt layer is moraine and then bedrock. Because the analysis only include the behaviour of the backwall, the underlying soil below the backfill is neglected.

6. DESIGN WITH CODE PROCEDURES

The design of the backwall of the bridges will first be executed with considerations to the Swedish codes and standards as well as the Finnish national annex, and appropriate loads and bending moments will be calculated. The loads from this chapter will then be used in the FE model, which is set up in Brigade/Plus.

6.1. Codes

The codes exists to help the engineer, and to give guidelines in design of structures. It states what loads to take into consideration and how the structure should be analysed. In Sweden there are a number of codes and regulations, and for bridges Eurocode, TRVK Bro 11 and TRVR Bro 11 applies.

6.1.1. Eurocode

The Eurocode (EC) is divided into 9 subsections, which then are divided further into subparts. A structure should be able to endure all loads and actions it is imposed by under its lifespan, and when designing a structure consideration of this is taken care of with partial coefficients (European Committee of Standardization, 2002a). For concrete structures both creep, shrinkage and second order theories, as well as design in ultimate limit state (ULS) and serviceability limit state (SLS), are of importance (European Committee of Standardization, 2005b).

When designing with regard to EC, and also the standards of the Swedish Road Administration, the partial coefficient method is used. In short, that means a partial coefficient is multiplied with every component to take care of uncertainties and to make it possible to combine loads.

6.1.2. Swedish Road Administration standards

As a complement for EC there are documents provided by the Swedish Road Administration with demands regarding bridge design. They are divided into different parts depending on the type of bridge, e.g. a road bridge or a railway bridge. The standards for road bridges are called TRVK Bro (*Trafikverkets tekniska krav Bro*) and TRVR Bro (*Trafikverkets tekniska råd Bro*)

and serves as a guidance for how EC should be interpreted. The documents works in collaboration with TRVFS 2004:31 and TRVFS 2004:43 (*Vägverkets föreskrifter*).

For example it states that all components of the bridge should be available for inspection in all times, and also how loads should be considered (Swedish Road Administration, 2011b). For design of the backwall, in consideration to earth pressure from the backfill soil, reference is made to TK Geo, which handles technical demands for geotechnical structures.

6.2. Loads

6.2.1. Permanent actions

Permanent actions are defined after their constant duration (European Committee of Standardization, 2002a). In TRVK Bro 11 all the permanent actions loading a bridge is listed, and some of them are (Swedish Road Administration, 2011b):

- Self-weight
- Earth pressure
- Displacement of support
- Shrinkage of concrete

In this dissertation, only the influence of the earth pressure will be handled further. In the FE model however, the self-weight is included in the analysis to serve as a verification that the mesh of the model is correct.

6.2.2. Variable actions

The variable actions, in contrary to the permanent actions, are actions that can vary in time and magnitude. TRVK Bro 11 also states the variable actions, and the ones that are of interest when designing the backwall with regard to horizontal forces are:

- Traffic load (braking load)
- Temperature
- Surcharge load

6.2.3. Earth pressure

Bridges in Sweden are designed for at rest earth pressure, and restrictions of the backfill soil is given in TK Geo (Swedish Road Administration, 2011b). The backfill soil should have properties so that the settlements won't be too large, therefore it is usually composed by blasted rock which is placed in layers, each compressed before putting on a new layer (Swedish Road Administration, 2011a). However, the backfill soil of Haavistonjoki Bridge is

discussed in chapter 5.4.1 above, and again presented in table 6.1 along with the earth pressure coefficients retrieved from eq. 4.2 and eq. 4.4.

Table 6.1. Backfill soil properties used to calculate the at rest earth pressure.

Blasted rock	**Parameter value**
Weight, γ_{bf}	$20\ kN/m^3$
Friction angle, ϕ'_{bf}	42°
Modulus of elasticity, E_{bf}	$50\ MPa$
At rest earth pressure coeff.	0,33
Passive earth pressure coeff.	5,05

The pressure from the backfill soil, on the backwall, varies with depth and are generated by a part of eq. 4.1:

$$p_{bf} = K_0 \gamma_{br} z = 0{,}33 \cdot 20 \cdot z = 6{,}6z\ kN/m^2$$

The distribution of the earth pressure is of a triangular shape, and depicted in figure 6.1, thus giving an earth pressure at the bottom of the backwall of:

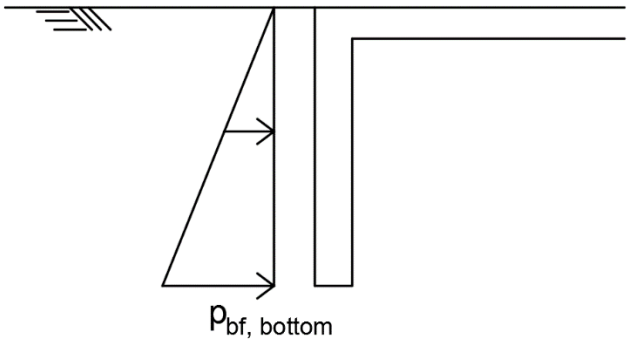

Figure 6.1. Earth pressure on the backwall from the at rest earth pressure.

$$p_{bf,bottom} = 6{,}6 \cdot H_{bw} = 6{,}6 \cdot 2{,}5 = 16{,}5\ kN/m^2$$

6.2.4. Traffic

The traffic load is defined as a variable load, and thus many different load models exist to compensate for the many different outcomes of traffic. The bridge in the dissertation are going to be designed for road traffic according to the standards TDOK 2013:0273 and TDOK 2013:0267. The two documents provides demands and advices regarding bearing capacity calculations for bridges and is an extension of the more general standards TRVK Bro and TRVR Bro.

The only traffic load contributing to the horizontal displacement of the backwall is the braking force, decided by section 2.3.2.3.1 in TDOK 2013:0267. The standard state that the braking force should be linearly interpolated between different braking forces corresponding to different bridge lengths, presented in table 6.2.

Table 6.2. Braking forces corresponding to different bridge lengths.

Bridge length	**Braking force**
$20\ m$	$70\ kN$
$40\ m$	$170\ kN$
$170\ m$	$470\ kN$

The bridge length is decided by the length between two joints that transfer horizontal forces. In the case of an integral bridge (i.e. a jointless bridge), the bridge length becomes the distance between the two ends of the backwalls, figure 6.2. For the Haavistonjoki Bridge, the distance between the backwall ends, and also the distance between the two points of the bridge transferring horizontal forces, is $51{,}2\ m$.

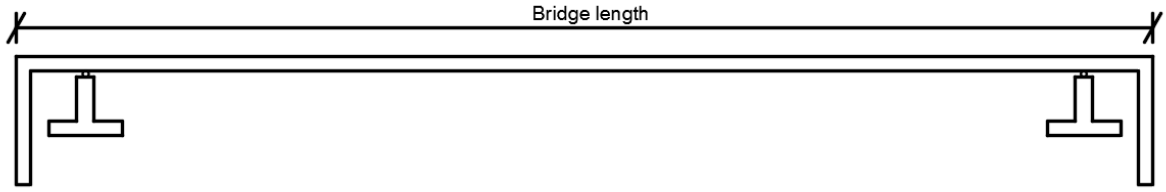

Figure 6.2. The distance between the two points transferring horizontal forces is equal to the bridge superstructure length.

The linearly interpolated value of the braking force is $F_{B,TRVK} = 196\ kN$. The force is assumed to be equally distributed over the whole width of the bridge, generating the force $q_{B,TRVK} = \frac{196}{11{,}5} = 17{,}04\ kN/m$. This force induces a resisting force acting on the backwall, eq. 6.1, with a value equal to the breaking force. The force can then be triangularly distributed, in the same manner as the earth pressure, over the height of the backwall. The force equilibrium is illustrated in figure 6.3.

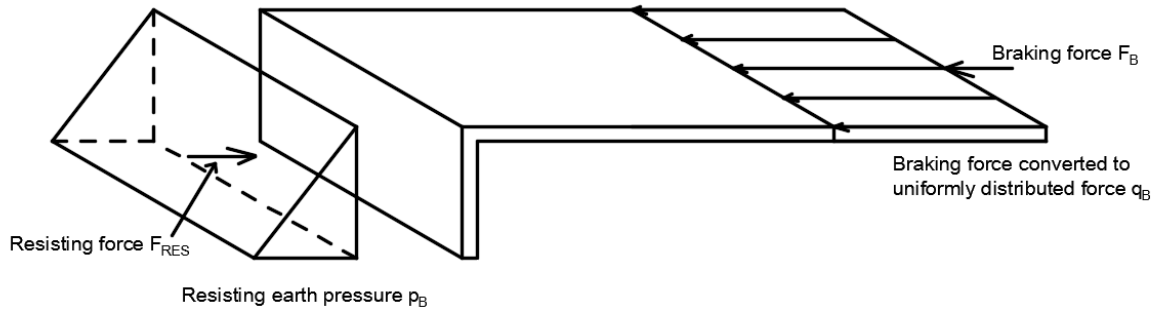

Figure 6.3. Force equilibrium of breaking force and resisting earth pressure used to calculate the earth pressure induced by breaking.

$$q_{resisting} = q_{B,TRVK} = p_{B,bottom} \cdot \frac{1}{2} \cdot H \tag{6.1}$$

$$p_{B,TRVK,bottom} = \frac{2 \cdot q_{B,TRVK}}{H_{bw}} = \frac{2 \cdot 17{,}04}{2{,}5} = 13{,}63\ kN/m^2$$

In the same way, the braking force calculated from the crane is used to calculate the resisting earth pressure at the bottom of the backwall.

$$q_{B,crane} = \frac{F_{B,crane}}{11{,}5} = \frac{220{,}8}{11{,}5} = 19{,}2\ kN/m$$

$$p_{B,crane,bottom} = \frac{2 \cdot q_{B,crane}}{H_{bw}} = \frac{2 \cdot 19{,}2}{2{,}5} = 15{,}4\ kN/m^2$$

6.2.5. Temperature

Temperature loads occur with varying temperature, when the structure is obstructed to move due to the layout without joints. The temperature loads should be calculated with respect to chapter 6 in SS-EN 1991-1-5 (European Committee of Standardization, 2003a). The change in temperature causing the largest expansion in the bridge is the temperature span between the highest annual temperature and the temperature at which the concrete was casted, assumed to be $T_0 = 10\ °C$. The annual temperatures are depending on the location of the bridge, and average values of Finnish temperatures are given in figures in the national annex and presented in table 6.3. The pages from the national annex of the Finnish Eurocode is found in appendix B.

Table 6.3. Air temperatures for the area around Tampere fetched from the Finnish NA of Eurocode.

Location	T_{max}	T_{min}
Tampere	$32\ °C$	$-38\ °C$

The temperature difference between the highest temperature and T_0 is $\Delta T = 32 - 10 = 22\ °C$. The thermal expansion coefficient for concrete $\alpha_{\Delta T} = 10 \cdot 10^{-6}\ /°\ C$. This gives the thermal strain of the bridge.

$$\varepsilon_{\Delta T} = \Delta T \cdot \alpha_{\Delta T} = 22 \cdot 10 \cdot 10^{-6} = 2{,}2 \cdot 10^{-4}$$

The thermal strain is multiplied with the thermal expansion length of the bridge to gain the displacement caused by the temperature change. Because the bridge expands and contracts equally in both directions over the bridge length, the thermal expansion length is equal to half of the distance between the ends of the two backwalls, $L_{exp} = 25{,}6\ m$.

$$\delta_T = \varepsilon_{\Delta T} \cdot L_{exp} = 2{,}2 \cdot 10^{-4} \cdot 25{,}6 = 0{,}00563\ m = 5{,}63\ mm$$

This deformation is then compared to a limit value according to TDOK 2013:0267. The limit value $\frac{H}{200}$, where $H = 2{,}5\ m$ is the height of the backwall, is $\frac{2{,}5}{200} = 0{,}0125\ m = 12{,}5\ mm$. As $0 < \delta < \frac{H}{200}$, the earth pressure due to the backwall movement by the temperature change takes the form:

$$p_T = p_0 + c_1 \delta_T \frac{200}{H} p_1 \tag{6.2}$$

where:

$p_0 =$ earth pressure at rest
$c_1 = 1$ when the earth pressure is unfavourable
$c_1 = 0{,}5$ when the earth pressure is favourable
$p_1 = p_p - p_0$ and $p_p =$ passive earth pressure

This is the reaction from the soil due to the thermal movements, when the backwall moves against the soil because of thermal expansion, and the earth pressure is assumed unfavourable. After inserting at rest earth pressure and passive earth pressure, and exploiting the common factoring, a new expression of eq. 6.2, dependent on the depth in the soil, is given.

$$\begin{gathered} p_0 = K_0 \gamma_{bf} z \\ p_p = K_p \gamma_{bf} z \\ p_T = \left(K_0 + \delta_T \frac{200}{H} \left(K_p - K_0 \right) \right) \gamma_{bf} z \end{gathered} \tag{6.3}$$

Values of the earth pressure coefficients and the weight of the soil are given in table 6.1, after inserting in eq. 6.3:

$$p_{T,EC} = \left(0{,}33 + 0{,}00563 \cdot \frac{200}{2{,}5} (5{,}05 - 0{,}33) \right) 20z = 49{,}13z\ kN/m^2$$

Now, the earth pressure at the bottom of the wall can be calculated, and the earth pressure due to the temperature expansion is showed in figure 6.4.

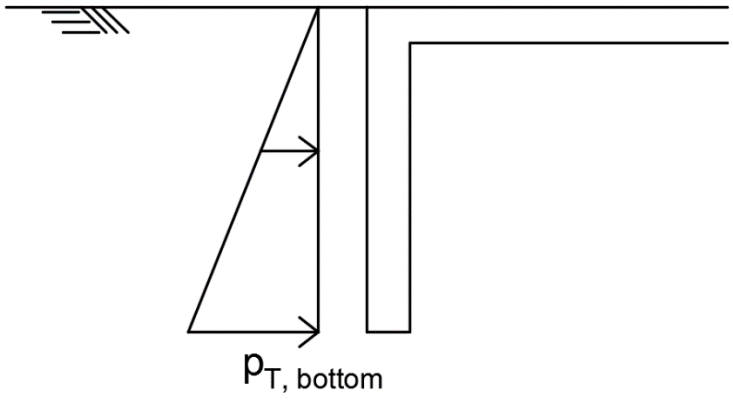

Figure 6.4. Earth pressure on the backwall from the temperature movements.

$$p_{T,EC,bottom} = 49{,}13 \cdot 2{,}5 = 122{,}8\ kN/m^2$$

The earth pressure and corresponding displacement from the measurements though, presents a temperature difference of only $\Delta T = (-2) - (-14) = 12\ °C$.

Again, the thermal expansion coefficient for concrete is $\alpha_{\Delta T} = 10 \cdot 10^{-6}\ /°\ C$, and the thermal strain of the bridge is:

$$\varepsilon_{\Delta T} = \Delta T \cdot \alpha_{\Delta T} = 12 \cdot 10 \cdot 10^{-6} = 1{,}2 \cdot 10^{-4}$$

The displacement caused by the temperature change.

$$\delta_T = \varepsilon_{\Delta T} \cdot L_{exp} = 1{,}2 \cdot 10^{-4} \cdot 25{,}6 = 0{,}00307\ m = 3{,}07\ mm$$

Again, the limit value $\frac{H}{200} = \frac{2{,}5}{200} = 0{,}0125\ m = 12{,}5\ mm$. Again $0 < \delta < \frac{H}{200}$, and the earth pressure due to the backwall movement by the temperature change in the measurement data takes the form as eq. 6.2. After inserting at rest earth pressure and passive earth pressure, and the values.

$$p_{T,meas} = \left(0{,}33 + 0{,}00307 \cdot \frac{200}{2{,}5}(5{,}05 - 0{,}33)\right) 20z = 29{,}79z\ kN/m^2$$

$$p_{T,meas,bottom} = 29{,}79 \cdot 2{,}5 = 74{,}5\ kN/m^2$$

6.2.6. Surcharge load

If a vehicle is standing on the road, beside the bridge, the load is taken up by the soil. The horizontal component of this load, decided by the earth pressure coefficient, will induce an active earth pressure on the bridge backwall, which in turn will cause a passive pressure in the other side. This type of load is called surcharge load, and the event is illustrated in figure 6.5.

The surcharge load is taken from the standards of Swedish Road Administration and is set to:

- $q_{SL} = 15\ kN/m^2$ for a width of 6 m of the road
- $q_{SL} = 10\ kN/m^2$ for the rest of the width

For the calculations in this dissertation, the surcharge load will be set to $15\ kN/m^2$ for the whole width for the sake of simplicity and with the argument that the main interest is to investigate the soil stiffness rather than design the backwall. The horizontal earth pressure caused by the surcharge load is calculated.

$$p_{SL} = K_0 \cdot q_{SL} = 0{,}33 \cdot 15 = 5{,}0\ kN/m^2$$

This pressure is of uniform magnitude over the whole depth according to figure 6.5.

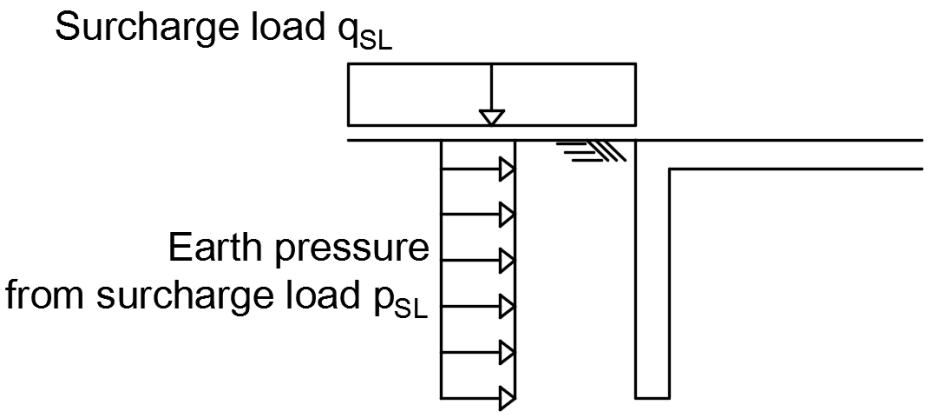

Figure 6.5. Earth pressure on the backwall from the surcharge load.

6.3. Section forces on the backwall

A common way is to consider the backwall as a cantilevering beam, with the fixed end at the top of the wall, subjected to a triangular load in case of earth pressure, braking force or temperature load, and a uniformly distributed load in case of surcharge load. The moment in the fixed end of the cantilevering beam corresponds to the moment e.g. used to design the reinforcement needed in the backwall.

The section forces for the load case depicted in figure 6.6 is obtained through force and moment equilibrium.

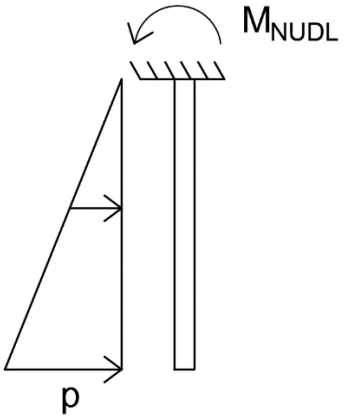

Figure 6.6. Section forces of a cantilevering beam with increasing load, e.g. lateral earth pressure.

$$M_{NUDL} = \frac{pH^2}{3} \tag{6.4}$$

where:

p = the pressure at the bottom of the backwall
H = the height of the backwall

The section forces the uniformly distributed load case for a cantilevering beam, depicted in figure 6.7, can be found in beam tables (Mårtensson & Isaksson, 2010).

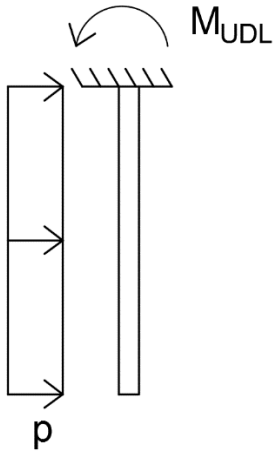

Figure 6.7. Section forces of a cantilevering beam with uniform load, e.g. surcharge load.

$$M_{UDL} = \frac{pH^2}{2} \tag{6.5}$$

The variables in the formulas above are the same as for the equations regarding the non-uniformly distributed load. The earth pressures from the different load cases are summarised in table 6.4.

Table 6.4. Summary of the earth pressures calculated above.

Load	**Earth pressure**
Earth pressure	16,5 kN/m^2
Braking force acc. to TRVK	13,6 kN/m^2
Braking force from the crane	15,4 kN/m^2
Temperature acc. to EC	122,8 kN/m^2
Temperature acc. to measurements	74,5 kN/m^2
Surcharge load	5,0 kN/m^2

Earth pressure
The section forces due to the at rest earth pressure:

$$M_{bf} = \frac{16{,}5 \cdot 2{,}5^2}{3} = 34{,}5\ kNm/m$$

Braking force
The section forces due to the braking force according to the standards of the Swedish road administration:

$$M_{B,TRVK} = \frac{13{,}6 \cdot 2{,}5^2}{3} = 28{,}4\ kNm/m$$

The section forces due to the braking force of the crane

$$M_{B,crane} = \frac{15{,}4 \cdot 2{,}5^2}{3} = 32{,}1\ kNm/m$$

Temperature
The section forces due to the temperature movements given by Eurocode:

$$M_{T,EC} = \frac{122{,}8 \cdot 2{,}5^2}{3} = 255{,}7\ kNm/m$$

The section forces due to the temperature movements from the measurement data:

$$M_{T,meas} = \frac{74{,}5 \cdot 2{,}5^2}{3} = 155{,}1\ kNm/m$$

Surcharge load
The section forces due to the surcharge load:

$$M_{SL} = \frac{5{,}0 \cdot 2{,}5^2}{2} 15{,}5\ kNm/m$$

The partial coefficients are disregarded in the calculations, this is because the loads are not going to be combined but it is only interesting to compare them separately. The full calculations of the loads and the section forces are included in appendix C.

7. COMPUTER MODEL

7.1. FE-modelling

The deformations of the backwall can be considered as small, thus a linear analysis is adequate. For small strains and linear analysis the use of the constitutive material relation Hooke´s law is applicable for isotropic materials (Timoshenko & Goodier, 1951). The parameters that affect the constitutive relation are the Young´s modulus E, the Poisson ratio ν, and in some cases also the shear modulus G. This approach will be valid when modelling the soil as a spring bed supporting the backwall.

However, the deformations in the soil may be considered as large, stating that when modelling the soil as a solid mass, a non-linear analysis must be performed (Pétursson, 2015). Then another constitutive relation have to be used taking into account the non-linear behaviour. The stresses and strains in the structure depends on the constitutive relation, and it is important to notice that with large deformations the volume may change (Krenk, 2009). The choice of elastic or elastic-plastic material in the analysis controls the outcome in such way that it determines what sort of analysis method and constitutive relation that is suitable for the calculations. A soil continuum is supposed to be an elastic-plastic material (Pétursson, 2015). This means that it can deform elastic up a certain limit, and then irreversible deformations also take place (Krenk, 2009).

A plate is a structural element characterised by that its thickness is much smaller than the other dimensions, e.g. width and height. The plate is loaded normal to its plane and for simplicity matters the coordinate system is symmetric about the local xy-plane and the thickness is symmetric about the local z-axis (Ottosen & Petersson, 1992). This will result in deformations in the local z-direction, and bending moments, twisting moments and shear forces. Both Bernoulli´s assumption for beam theory[2], Hooke´s law and plane stress is valid for plates subjected to loads giving small strains (Ottosen & Petersson, 1992). Because of the fact that the plate is only loaded normal to the plate, no horizontal resultants occur, i.e. no normal forces in the mid-plane, and thus there are no strains in the mid-plane.

If, however, the mid-plane is deformed and thus the strains in the mid-plane are nonzero, a feature called membrane action will occur. Then the structure will behave like a shell structure, where membrane actions are evident. The shell element can be seen as a structure that combines plate and plane stress theory (Ottosen & Petersson, 1992). This is the case for the frame bridge superstructure, with both vertical forces, due to e.g. self-weight and traffic, and horizontal forces, due to e.g. thermal actions.

[2] Plane sections remain plane

It is important to notice that FE-analysis of the mathematical model is an approximation and the process can be assumed to evolve from a physical problem, through a mathematical model, boundary conditions and loads, and end in results by selecting a sufficient mesh size (Chapelle & Bathe, 2011).

7.2. Brigade/Plus

Brigade/Plus is a computer program from Scanscot Technology, a Sweden based company with focus on advanced finite element analysis. The solver technology of Brigade is based on another well-known FE-program, ABAQUS, and the interface of the two programs are very alike. Brigade's main focus is analyses of bridges, but other structures may as well be analysed.

Some of the main features of the program consists of defining different parts and elements, which then can be assembled together. Every part is assigned a material, with properties defined by the user. Both linear and non-linear analyses can be performed. Then steps, loads and interactions between the structural elements is defined, as well as boundary conditions that needs to be defined. Brigade can interact with both Eurocode and the Swedish Road Administration codes, and e.g. load combinations and vehicles can be implemented directly into a model database (Scanscot Technology, 2015). Brigade/Plus Version 6.1-8 is used for the project, and the process of setting up the model will be described as follows.

7.3. Model of the bridges

7.3.1. Bridge geometry, section properties and steps

The bridge slab and backwalls are set up as planar shell elements. The shell elements look the same for the both models, and are shown in figure 7.1. The wingwalls are not included in the analysis due to the lowering effect they have on the earth pressure, i.e. excluding them will give a result on the safe side.

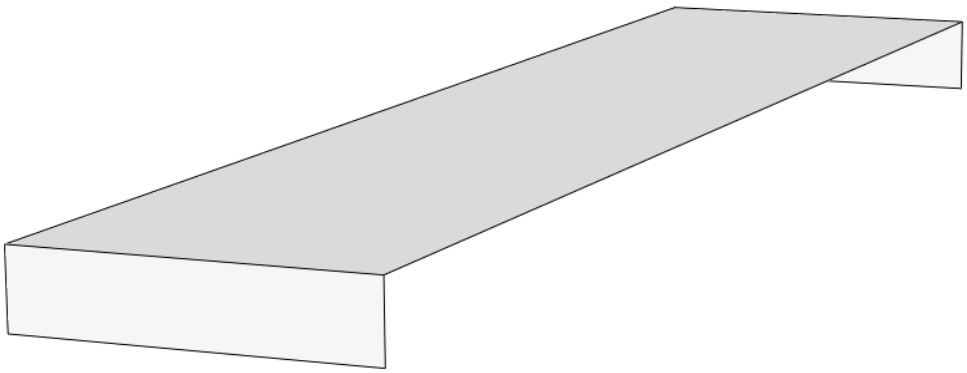

Figure 7.1. The geometry of the shell sections of the models.

To create the columns and piles, firstly a partition of the bridge slab is made to find the positions of the points of the columns. The setup of the bridge slab partition is different for the two bridge types because the columns have a slightly different placement (the semi-integrated bridge have intermediate columns at the backwalls). The partition lines are shown in figure 7.2 and figure 7.3. Then datum points are created at the end positions of the columns, by offsetting datum points from the intersections of the partition lines, and thereafter the datum points are bounded by wires, figure 7.4. The upper points of the end columns of the semi-integrated bridge are created $0{,}5\ m$ below the bridge slab, as shown in figure 7.4, to be able to create a constraint, this will be handled later in the chapter. The upper point of the mid columns however, are located on the surface of the slab, which allows the model to see it as a rigid connection.

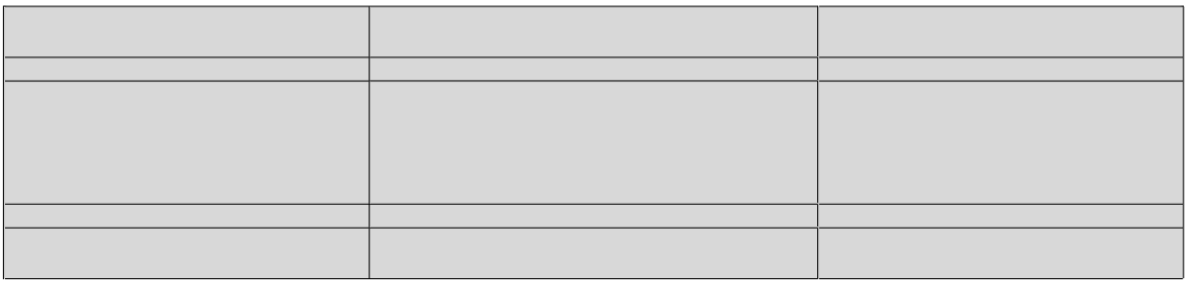

Figure 7.2. The partition lines of the bridge slab for the fully integrated abutment bridge.

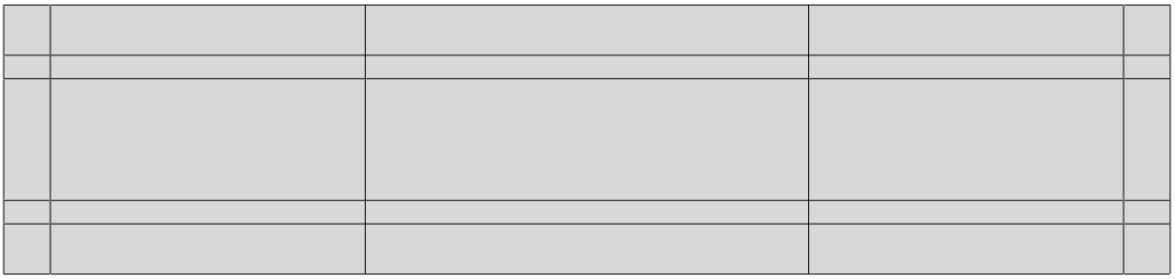

Figure 7.3. Partition lines of the bridge slab for the semi-integrated abutment bridge, notice the difference between the two models concerning the placement of the outer columns, instead of piers located at the backwall bottom.

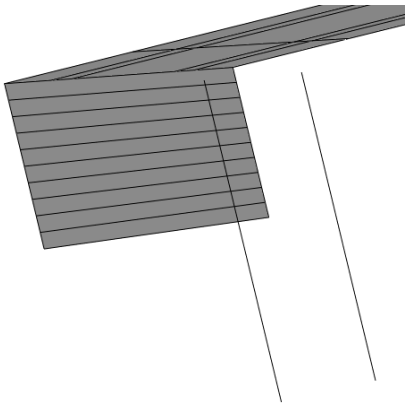

Figure 7.4. The location of the upper part of the outer columns of the semi-integrated abutment bridge are located below the surface of the bridge slab.

The parameters used when creating the material are density, Young's modulus, Poisson's ratio and the thermal expansion coefficient found in table 7.1. Then the sections are created for all the structural elements, where the thickness and material properties are defined, and assigned to the parts. The sections are created with the dimensions described in table 7.2 below.

Table 7.1. Material properties of the bridges, for concrete C35.

Material parameter	**Value**
Density, γ_c	$24\ kN/m^3$
Young's modulus, E_c	$34\ GPa$
Poisson's ratio, ν	0,2
Thermal expansion coefficient, $\alpha_{\Delta T}$	$1 \cdot 10^{-5}$

Table 7.2. Dimensions and element types of the different components of the bridges.

Part	**Cross sectional shape**	**Dimension**	**Type**
Bridge slab, thick area	Rectangular	$t = 0{,}86\ m$	Shell
Bridge slab, thin area	Rectangular	$t = 0{,}35\ m$	Shell
Backwall	Rectangular	$t = 0{,}735\ m$	Shell
Column	Circular	$d = 1\ m$	Wire
Piles	Circular	$d = 0{,}711\ m$	Wire

A material orientation is defined for the bridge slab and backwalls, oriented from a local coordinate system of the bridge slab and backwalls respectively. In the same way, a beam section orientation is defined for the columns and piles. The material orientation of the bridge slab and the backwalls is shown in figure 7.5, these orientations are important to consider when viewing the results.

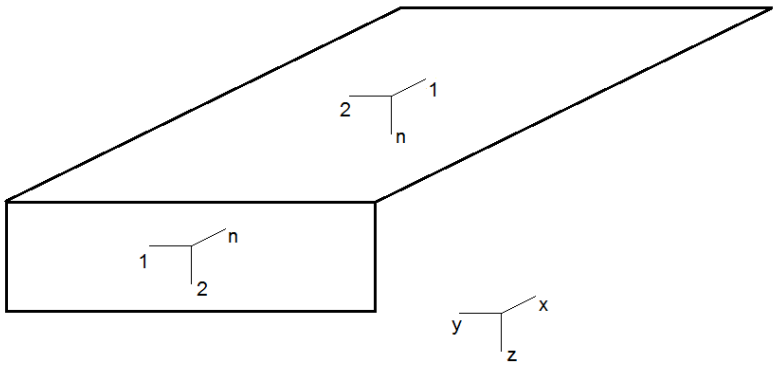

Figure 7.5. The material orientations of the bridge slab and backwalls, along with the global coordinate system.

The whole bridge is assembled together choosing independent meshing, and a step for each load is created as static linear perturbation.

7.3.2. Stiffness of the backfill soil

The interactions serves to define how the different structural elements work together. The backwalls are connected to the ground using spring to ground, where the spring stiffness calculated below is used. The spring stiffness is applied in the global X direction, i.e. in the longitudinal direction of the bridge.

The stiffness of the backfill soil is, as described earlier, often modelled as springs (either liner or nonlinear) where the stiffness k may be found from the displacement of the backwall and the magnitude of the horizontal load, cf. the general formula for spring stiffness:

$$k = \frac{F}{\delta} \tag{7.1}$$

For this project however, an initial stiffness is chosen equal to the at rest earth pressure coefficient, $k_{init} = K_0 = 0{,}33\ MPa$. Also, the stiffness of the soil is assumed to vary linear with the depth, increasing from zero at the top of the backwall, to k_{init} at the bottom, shown in figure 7.6.

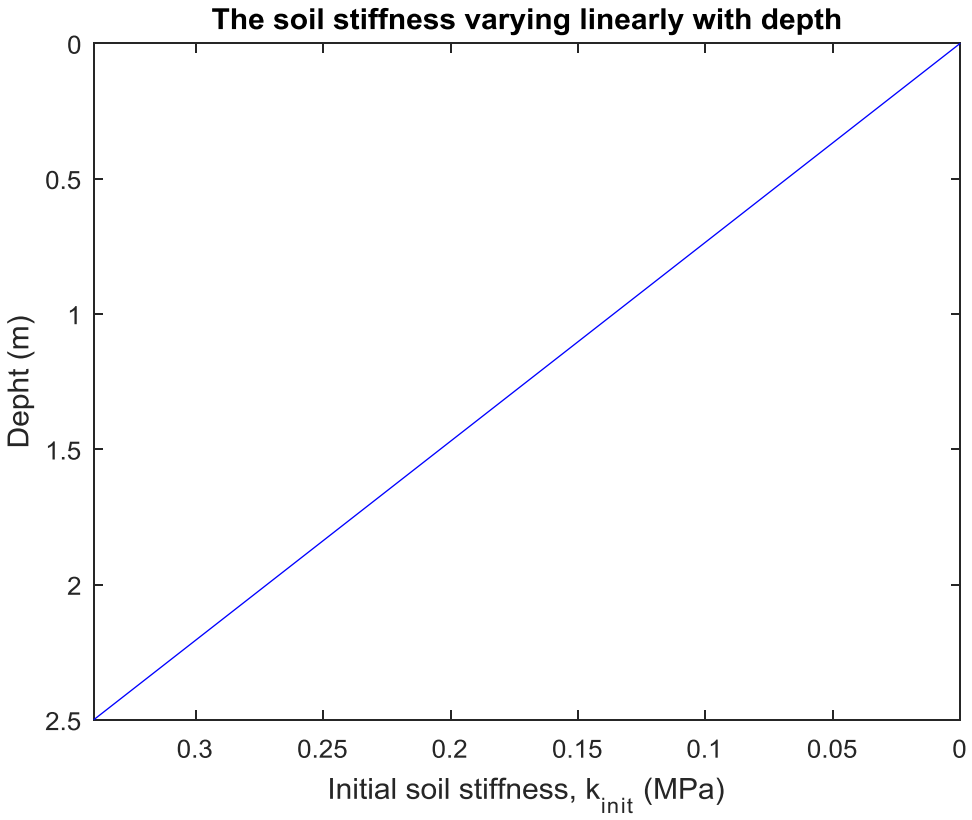

Figure 7.6. The curve shows how the soil stiffness varies with the depth at the surface of the backwall.

However, to implement the varying soil stiffness in the FE model in Brigade, the backwall must be divided into segments containing constant stiffness. The backwall is divided into 10 levels with the height $0{,}25\ m$ each, containing constant stiffness through its thickness. The

soil stiffness used for each level is presented in table 7.3, along with the depth to the centre of each level.

Table 7.3. The centre of the levels and the corresponding initial stiffness at the level.

Depth (m)	**Soil stiffness,** k_{init} (MPa)
0,125	0,033
0,375	0,066
0,625	0,099
0,875	0,132
1,125	0,165
1,375	0,198
1,625	0,231
1,875	0,264
2,125	0,297
2,375	0,330

The variation of the stiffness used in the FE model is also shown in figure 7.7.

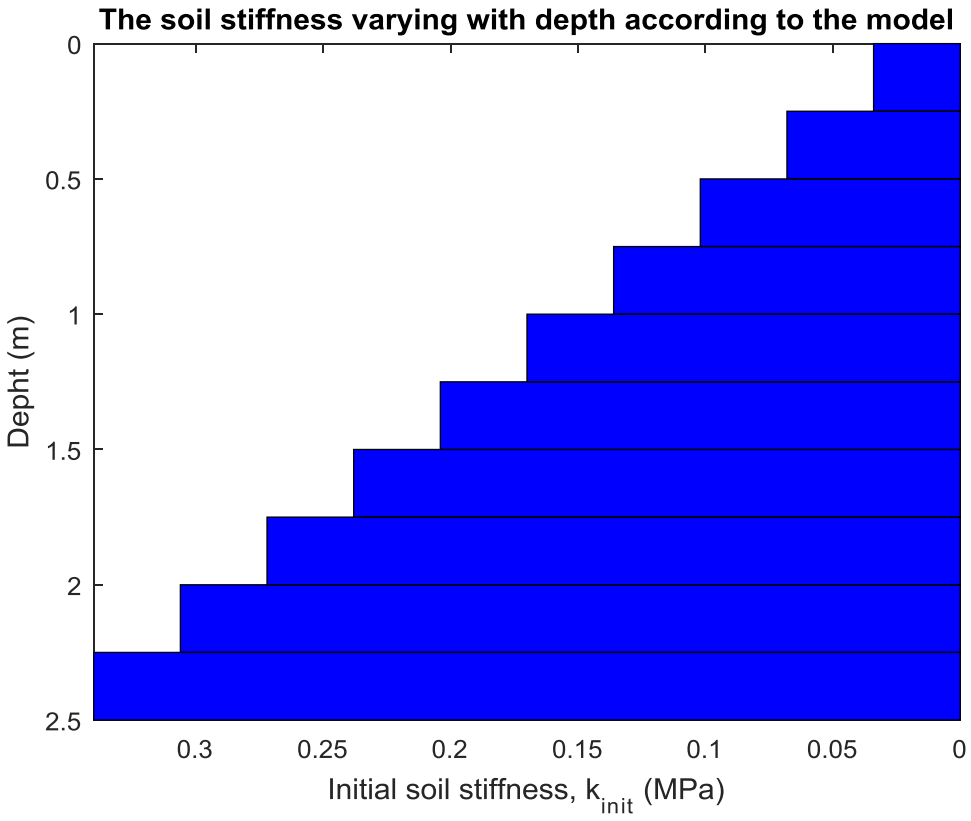

Figure 7.7. Soil stiffness variation with the depth at the surface of the backwall.

Then the deformations caused by the loads with this stiffness applied are going to be compared to the deformations retrieved from the measurement data.

7.3.3. Other interactions

Pile to backwall
For the fully integrated bridge, the piles are connected to the backwalls using the interaction tie, which allows the top of the piles to deform and displace in the same manner as the backwall. This interaction is used because the piles are rigidly connected to the backwall. Figure 7.8 illustrates how the tie is connected between the top of the piles and the whole backwall.

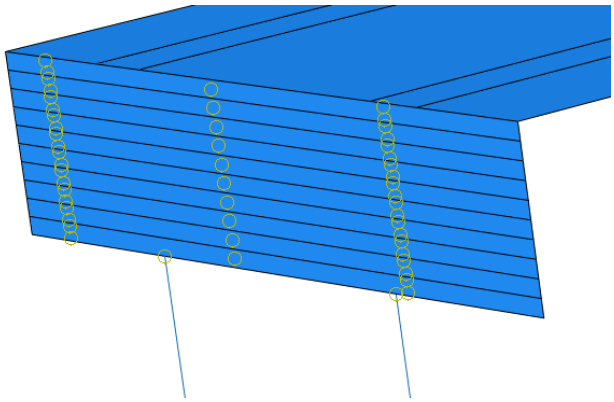

Figure 7.8. The tie interaction between the pile tops and the whole backwall.

Bearings
The bearings are created as an interaction between the outer columns and the bridge superstructure. The interaction type used is coupling, which means that the both points will interact in the same way and movements can be prescribed. To characterise a bearing, the coupling is locked in the vertical and transversal direction, along with the rotations, and set free to move and rotate in the longitudinal direction of the bridge.

7.3.4. Defining loads and boundary conditions

The self-weight is applied as a gravity force, defined by the gravity constant $g = 9{,}81\ m/s^2$.

The earth pressure is applied as a hydrostatic pressure, increasing from 0 at the backwall top to $p_{bf} = 17\ kN/m^2$ at the backwall bottom. In the same way the surcharge load is applied, but as a constant pressure, acting on the backwalls with the value $p_{SL} = 5{,}1\ kN/m^2$.

The braking force is applied as a surface traction, acting in the plane of the bridge slab, in the parallel direction of the edge of the bridge slab and distributed over the whole slab area, through dividing it with the length and width of the bridge. The pressure from the load calculated from the measurement data in chapter 5 is used for the iteration of the stiffness, $p_{B,crane}$. The braking force from the Swedish standard is then used for comparison, $p_{B,TRVK}$.

$$p_{B,crane} = \frac{220{,}8}{51{,}2 \cdot 11{,}5} = 0{,}375\ kN/m^2$$

$$p_{B,TRVK} = \frac{196}{51{,}2 \cdot 11{,}5} = 0{,}333\ kN/m^2$$

The temperature is applied to the bridge slab as a predefined field. Usually, the temperature difference between two extreme temperatures, and the temperature in which the bridge is casted is defined, and two steps, *tempHigh* and *tempLow*, is used. But in the case of updating the model through the measurement data, the same temperature difference used in the calculations above is used, i.e. $\Delta T = 12\ °C$, and for comparison with Eurocode, $\Delta T = 22\ °C$. Figure 7.9 show the temperature field for the Haavistonjoki Bridge.

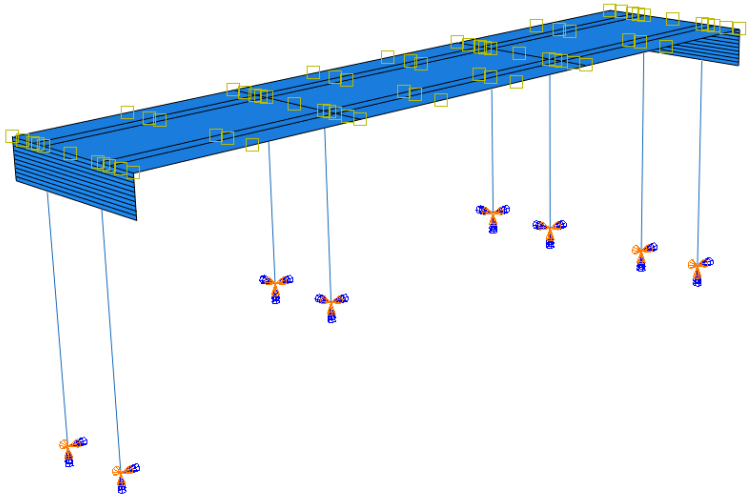

Figure 7.9. The field chosen for the temperature field of the fully integrated bridge (Haavistonjoki Bridge). Note that the piles, backwalls and columns are not included as the largest temperature difference will occur in the bridge slab.

The boundary conditions are applied at bottom of the columns, to characterise the spread foundations, and thus prevent the structure from moving in the wrong way. All the translations and rotations are prescribed. For the piles, the boundary condition at the end of the pile is prescribed translation and rotation in all directions except rotation about the y-axis.

For the semi-integrated abutment bridge, the boundary conditions are set with prescribed rotations and displacements in all directions and for all columns.

Figures 7.10 and 7.11 shows the final appearance of the models of the two bridges, before being meshed.

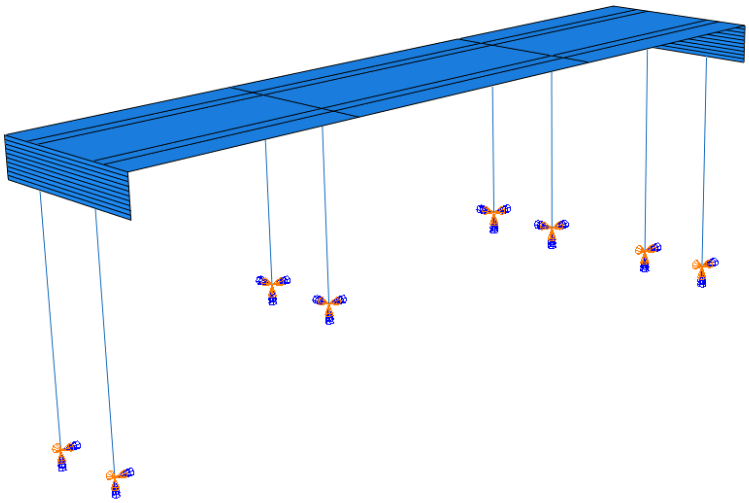

Figure 7.10. Final geometry of the fully integrated model of Haavistonjoki Bridge

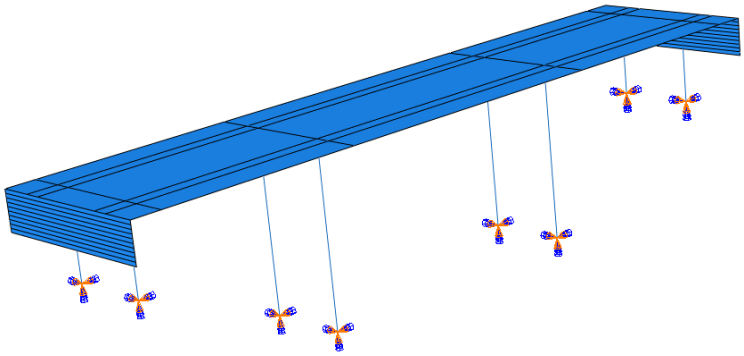

Figure 7.11. Final geometry of the semi-integrated model

The loads and boundary conditions used in the model are summarized in table 7.4.

Table 7.4. Explanation to the loads and boundary conditions used in the models.

Load/BC	**Magnitude**	**Type**	**Field**
Self-weight	$g = 9{,}81\ m/s^2$	Gravity load	Whole model
Earth pressure	$17\ kN/m^2$	Hydrostatic pressure	Backwalls and wingwalls
Breaking force	$0{,}333\ kN/m^2$	Surface traction	Bridge slab
Surcharge load	$5{,}1\ kN/m^2$	Pressure	Backwalls and wingwalls
Temperature diff.	$\Delta T = 12\ °C$	Predefined field	Whole model (except piles)
Columns to ground		Rigid	Bottom point of columns
Piles to ground		Rigid	Only allowing rotation about y-axis

7.3.5. Meshing of the models

The mesh is set as structured, and with quad shaped elements.

7.3.6. Verification of the model

Sufficient mesh size
The mesh size is iterated until a sufficient mesh size is found. This is done by comparing the bending moment of the bridge slab for some different sizes; 0,1, 0,2, 0,3 and 0,4. The values of the bending moment is found through free body cut, initiated in the Mesh module, and the results are presented in figure 7.12.

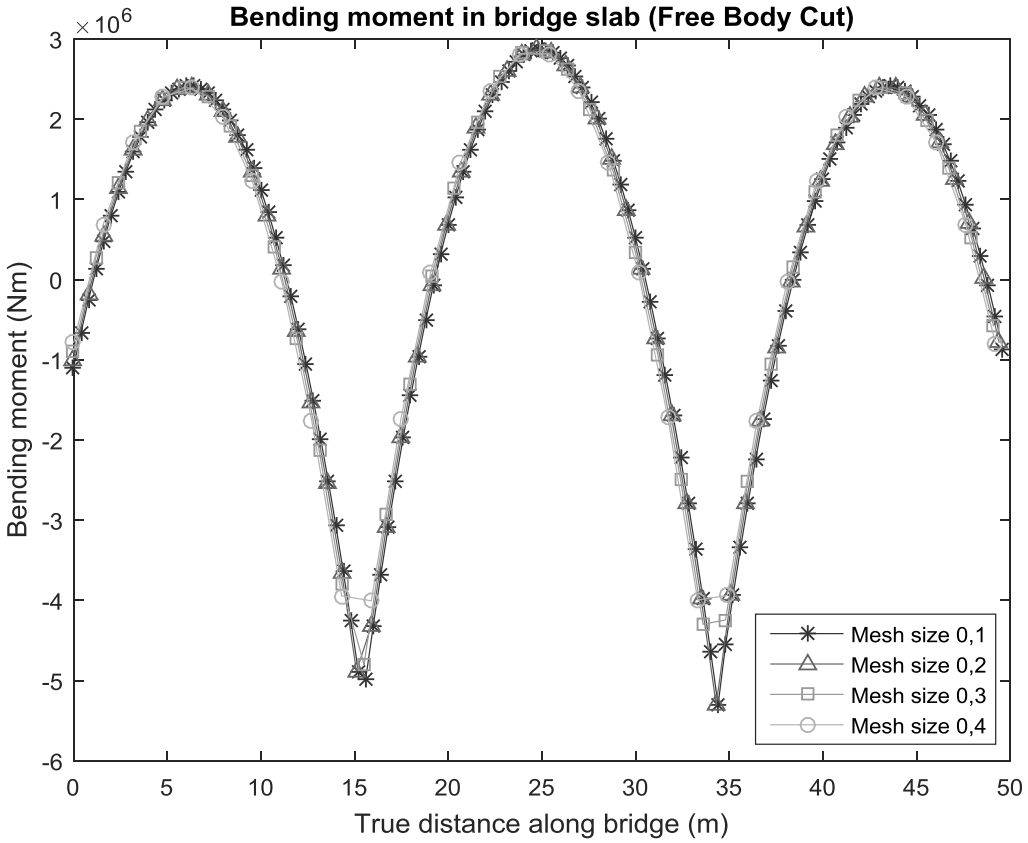

Figure 7.12. Curves showing the variation of the bending moment in the bridge slab due to different mesh size.

From the figure, it is visible that the bending moment converges at the sizes 0,2 and 0,1. A mesh size of 0,2 is therefore adequate.

8. CALIBRATION OF THE MODEL DUE TO THE MEASUREMENT DATA

The soil stiffness from the measurement data is obtained through dividing the earth pressure difference by the displacement. From table 5.2, the difference in earth pressure and the displacements are given for the two abutments due to the temperature change, and for the eastern abutment due to the braking of the crane. The soil stiffness on the middle level of the backwall is calculated with eq. 8.1 and presented in table 8.1.

$$k_s = \frac{\Delta p}{\delta} \tag{8.1}$$

Table 8.1. The predicted earth pressure of the middle level of the backwall, determined from the measurement data.

Load case	**Soil stiffness, k_s ($MN/m/m^2$)**
Temperature (T4)	16,23
Temperature (T1)	191,67
Braking (T4)	100

It is noticeable how big the difference is between the eastern abutment (T4) and the western abutment (T1). This means that the backfill soil on the two ends of the bridge does not have equal stiffness.

The FE model is updated with the stiffness gained from the measurement data, and the displacements from the FE model and the measurement data are compared. As the initial value of the iteration step, the stiffness from table 8.1 is set as the maximum stiffness, i.e. acting on the bottom of the backwall, assuming a linear increase with depth as before. The maximum value of the stiffness is then increased stepwise, and presented in tables.

Iteration of the stiffness due to the temperature change

The stiffness is iterated taking into consideration the ground conditions, i.e. the difference in displacement of the two abutments. The soil stiffness at the western backwall (T4) is set constant during the iterations with the value $k_{T,T4,middle} = 16\ MN/m$, and the soil stiffness at the other abutment is increased until the displacements reaches the limit values, $\delta_{lim,T,T4} = 5{,}3\ mm$ and $\delta_{lim,T,T1} = 0{,}3\ mm$ at the depth of $z = 0{,}15\ m$. The reason why the earth pressure is set constant at the weaker side is that the change of earth pressure will not be simultaneous due to the difference in soil stiffness.

Figure 8.1 presents the displacement of the eastern backwall (T4) and figure 8.2 presents the displacement of the western backwall (T1). The dashed line represents the limit displacement.

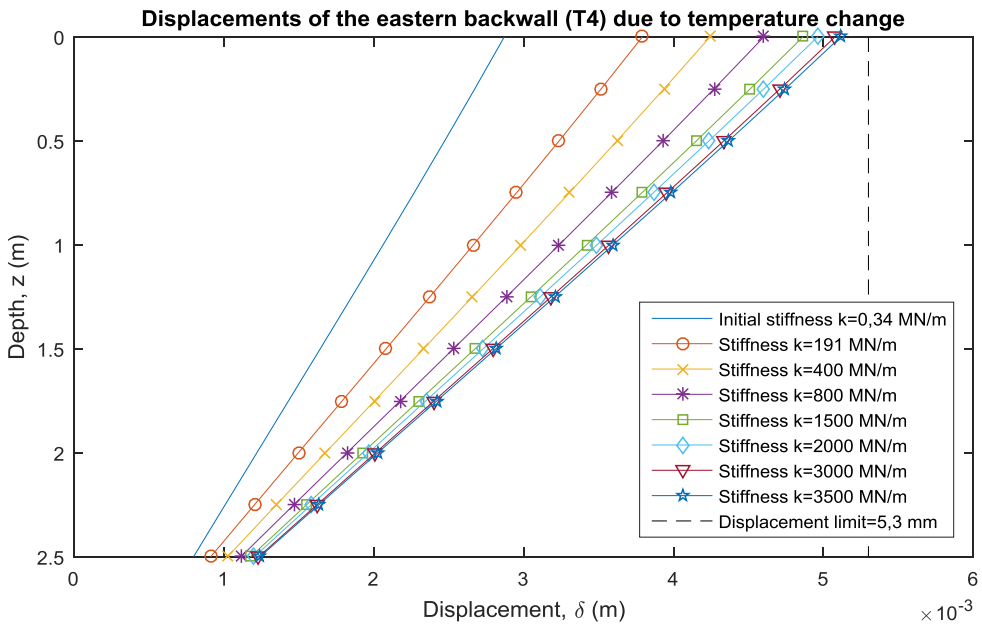

Figure 8.1. Displacements of backwall T4 due to the temperature change, the limit displacement is not reached.

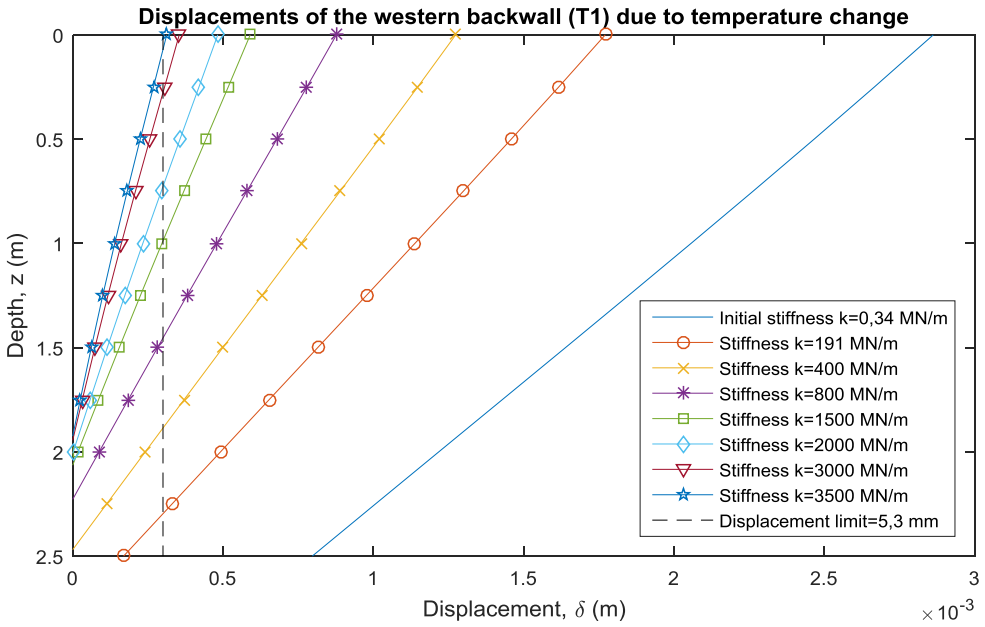

Figure 8.2. Displacements of backwall T1 due to the temperature change, the limit displacement in reached for a very high stiffness.

The values of the soil stiffness in the figures is the stiffness at the middle level of the backwall, increasing linearly from 0 at the top of the backwall to a maximum value at the bottom as presented in section 7.3.2. As it turns out, the displacement does not reach the limit within a reasonable stiffness for the eastern backwall, but reaches the measured displacement at the western backwall.

The middle level stiffness and corresponding displacements at the measured level on the backwall are presented in table 8.2.

Table 8.2. Summary of the iterations of the stiffness due to the temperature change.

Stiffness, $k_{T,T4}\ (MN/m)$	Stiffness, $k_{T,T1}\ (MN/m)$	Displacement, $\delta_{z=0,15\,m,T4}\ (mm)$	Displacement, $\delta_{z=0,15\,m,T1}\ (mm)$
0,34	0,34	2,75	2,75
16	95,5	3,63	1,67
16	200	4,06	1,20
16	400	4,40	0,82
16	750	4,65	0,55
16	1000	4,74	0,44
16	1500	4,86	0,32
16	1750	4,90	0,29

Even though the results from the iteration does not reach the limit displacement on abutment T4, for the continuous calculations the soil stiffness at the two abutments is set to $k_{T,T4} = 16\ MN/m$ and $k_{T,T1} = 1750\ MN/m$.

Iteration of the stiffness due to the braking force

The first value of the iteration of the middle stiffness is set to $k_{B,T4} = 50\ MN/m$ at the eastern backwall. As for the temperature change, the stiffness at one of the backwalls is set constant and the other side is increased. The same reason as above yields, with the addition that now active earth pressure arise at the side that is set constant. The western backwall (T1) is given the stiffness $k_{B,T1,middle} = 100\ MN/m$, and the displacements of the eastern backwall is presented in a figure showing the steps of the iteration. Figure 8.3 illustrates the displacements of the backwall, the dashed line represents the final displacement wanted in at the top region of the backwall, $\delta_{lim} = 0{,}03\ mm$.

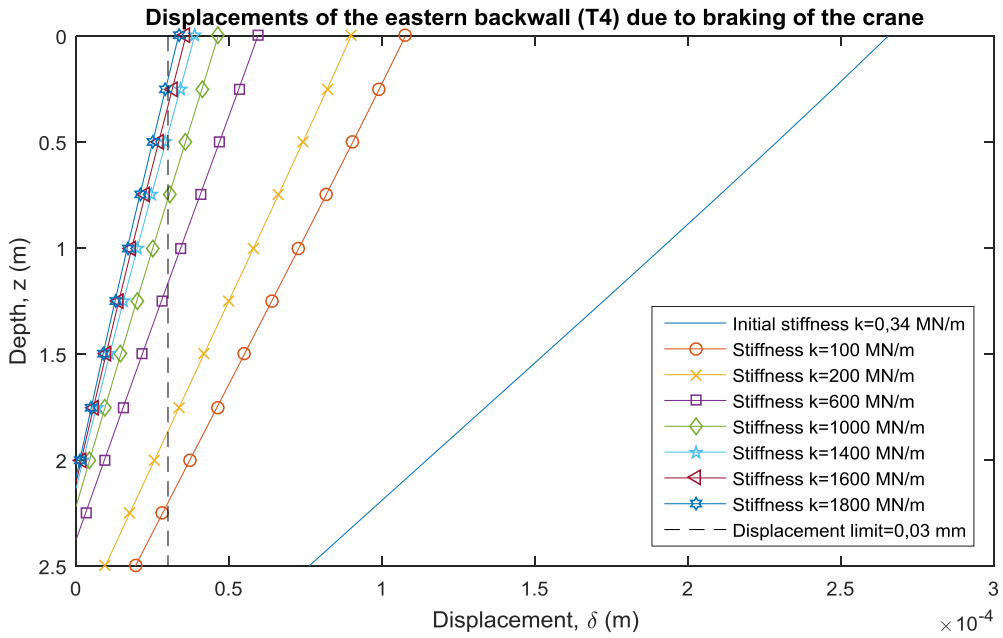

Figure 8.3. Displacements of backwall T4 due to the braking force from the crane, the limit displacement in reached for a very high stiffness.

The maximum values of the stiffness and the corresponding maximum displacements are also presented in table 8.3.

Table 8.3. Summary of the iterations of the stiffness due to the braking of the crane.

Stiffness, $k_{B,T4}$ (MN/m)	Displacement, $\delta_{z=0,15m}$ (mm)
0,34	0,254
50	0,102
100	0,085
300	0,055
500	0,043
700	0,036
800	0,033
900	0,030

According to figure 8.3 and table 8.3, the stiffness which have the displacement limit of $\delta_{B,lim} = 0{,}03\ mm$ is $k_{B,T4} = 900\ MN/m$ and $k_{B,T1} = 100 MN/m$.

Unfortunately, the stiffness required to reach the measured displacement for the two load cases are very high compared to the predicted stiffness calculated from the measurement data. This is probably because something is wrong with the measurement data or an assumption in the model. For example the braking test only provided earth pressure in one point (measurement point K) on the backwall. Also the measurement of the earth pressures from the temperature change seems to be varying much over the points of measure. Another uncertainty is what is happening regarding the earth pressure, and hence the soil stiffness, at the side that is set constant during the analysis.

An interesting fact though, is that the iterated soil stiffness is 9 times higher than the predicted for both the temperature and the braking case.

9. RESULTS AND DISCUSSION

The results of the iterations in the previous chapter are presented in figure 9.1 and 9.2, as well as in table 9.1. In the table, the final values of the iteration are compared to the predicted values of the stiffness, calculated from the earth pressure and the displacement assembled during the measurement of the bridge.

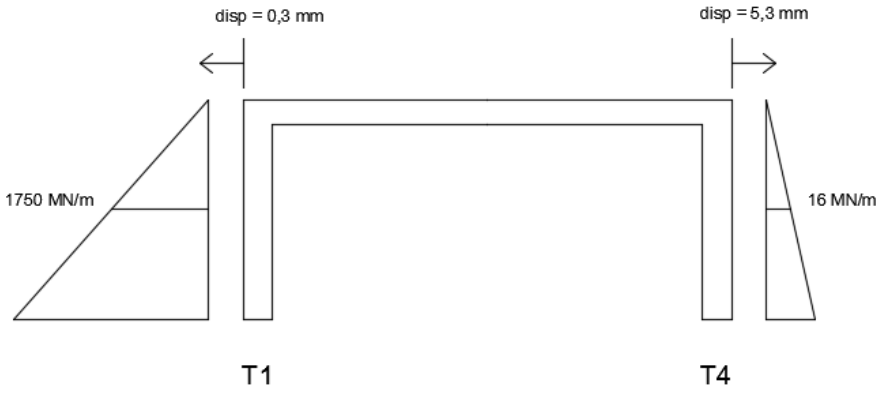

Figure 9.1. Iterated stiffness at the middle of the backwalls and the limit displacements for the temperature movements.

Figure 9.2. Iterated stiffness at the middle of the backwalls and the limit displacements for the braking of the crane.

Table 9.1. The predicted soil stiffness calculated from the measurements compared to the iterated value for different load case and abutment.

Load case	**Predicted stiffness**	**Stiffness from iteration**
Temperature (T4)	$16{,}23\ MN/m$	$16\ MN/m$
Temperature (T1)	$191{,}27\ MN/m$	$1750\ MN/m$
Braking (T4)	$100\ MN/m$	$900\ MN/m$

As discussed in the previous chapter, the iterated stiffness is much larger than the predicted, due to errors either in the model assumptions or the measurement data. Although, this stiffness is inserted in the FE models to retrieve the bending moments in the backwall given by the measured displacement.

The stiffness at backwall T4 due to the braking force is much larger than the stiffness due to the temperature movement at the same backwall, as seen in table 9.1. This is because the braking load is a fast load, giving an impulse to the backfill soil. This impulse will only generate a small displacement, hence increasing the stiffness calculated from eq. 8.1. On the contrary, the temperature expansion is a slow and locked deformation, generating larger displacements and hence lower value of the stiffness. The loads corresponding to the fast loading is the braking force and the surcharge load, and the loads corresponding to the slow loading is the temperature movements and the at rest earth pressure.

9.1. Haavistonjoki Bridge

Temperature expansion
The bending moments due to the loads corresponding to the slow loading for the eastern backwall (T4) are compared to each other in figure 9.3.

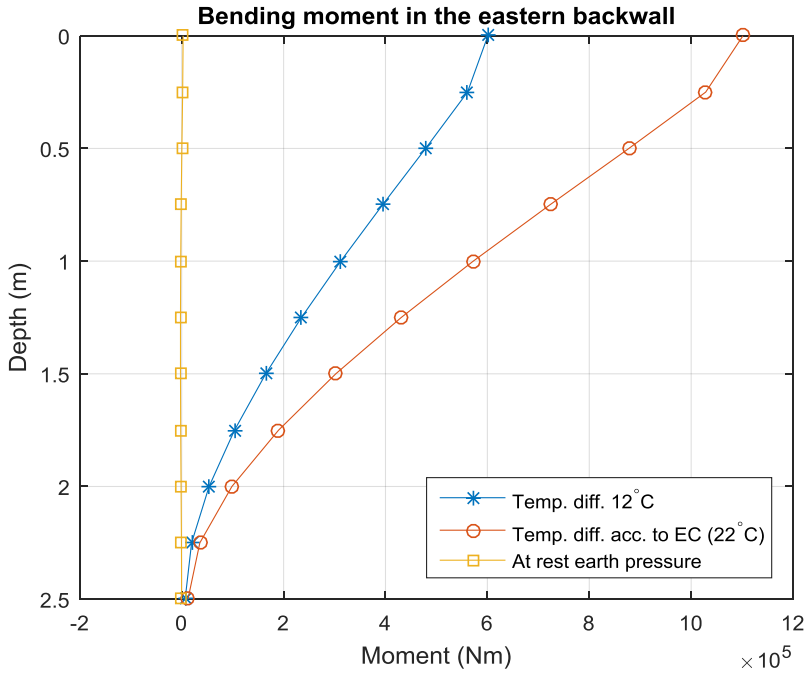

Figure 9.3. The bending moments of the eastern backwall (T4) plotted in the same figure for comparison.

The different shapes of the curves is depending on the varying magnitude of the loads. The springs between the backwall and the soil is capable of withstand the earth pressure, providing a spring support, but not for the temperature movements.

At the western backwall (T1), the results differs due to much more stiff soil is presented in figure 9.4.

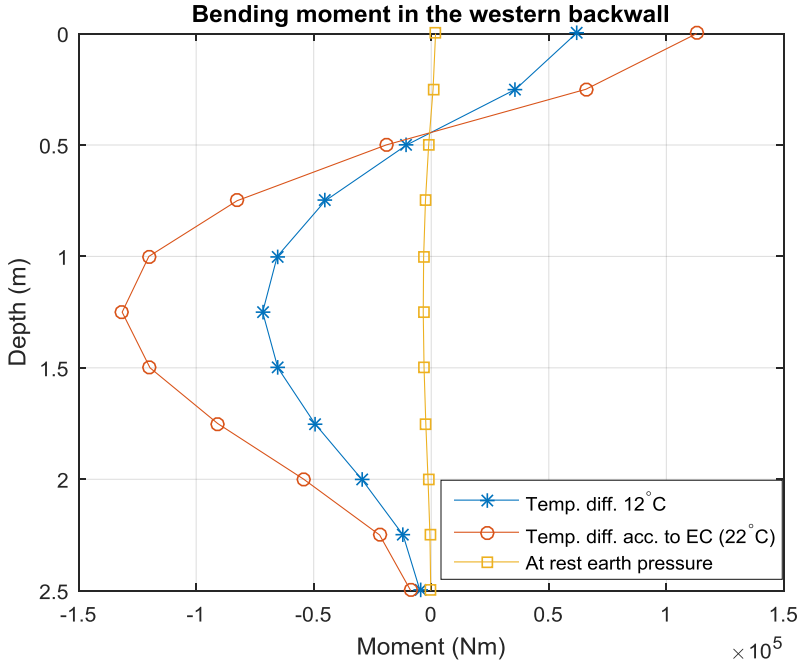

Figure 9.4. The bending moments of the western backwall (T1) plotted in the same figure for comparison.

The difference in shape of the moment curves of the western and the eastern backwall is due to the difference in soil stiffness. The backwall supported by the weak soil behaves much like a cantilevering beam for the large loads, and the backwall supported by the stiff soil behaves like a beam on an arbitrary number of spring supports, the load cases are illustrated in figure 9.5.

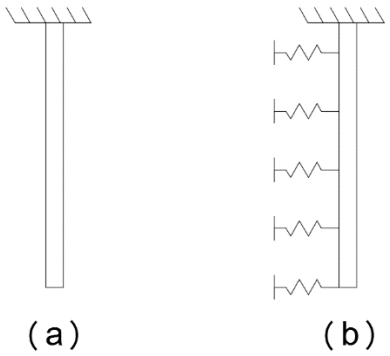

Figure 9.5. (a) The backwall behaves like a cantilevering beam when subjected to large loads in weak soil. (b) The backwall behaves like a beam on spring supports when subjected to loads in stiff soil.

Braking force

The bending moments due to the loads corresponding to the fast loading for the eastern backwall (T4) are compared to each other in figure 9.6.

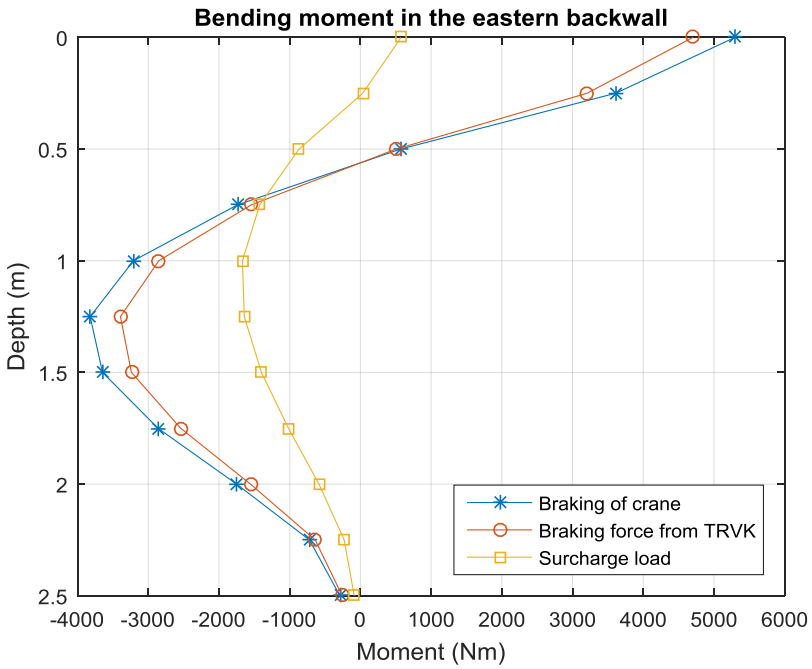

Figure 9.6. The bending moments of the eastern backwall (T4) plotted in the same figure for comparison.

The same discussion about the spring support is applicable on the fast loads. The soil in the braking analysis is less stiff than for the temperature movements, but the loads are smaller as well.

9.2. Semi-integrated bridge

Temperature expansion

In the same way, moment curves are provided for the semi-integrated bridge, presented in figures 9.7 and 9.8 for the temperature movement.

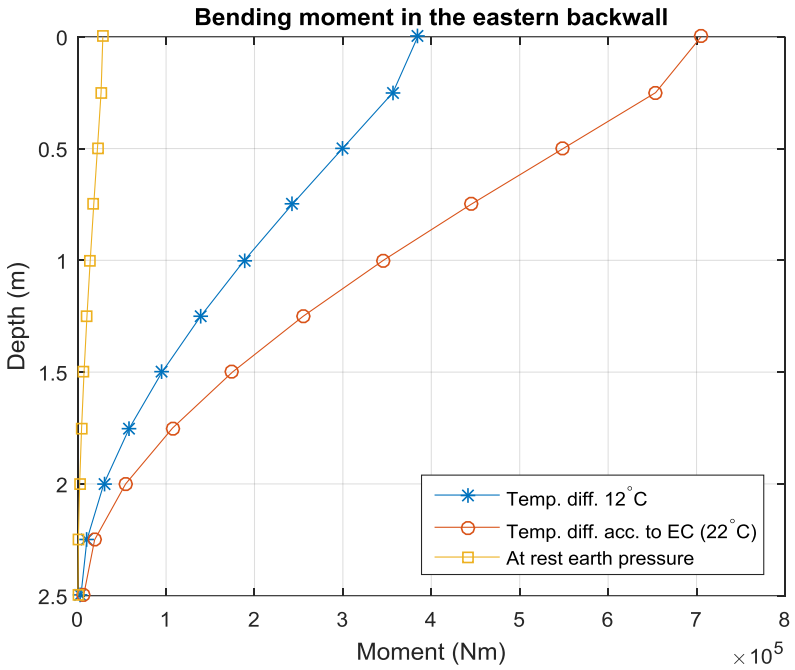

Figure 9.7. The bending moments of the eastern backwall (T4) plotted in the same figure for comparison.

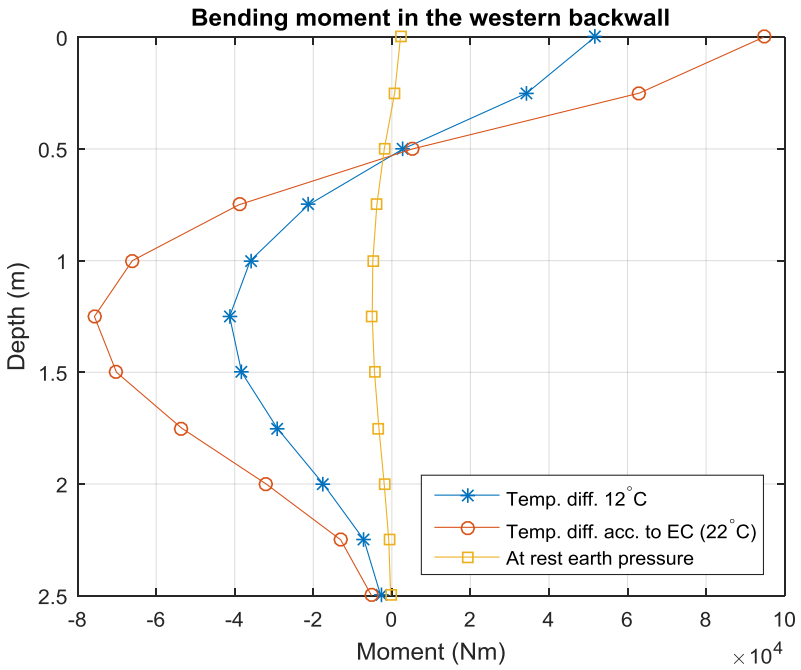

Figure 9.8. The bending moments of the western backwall (T1) plotted in the same figure for comparison.

Braking force

Moment curves are also provided for the braking load and the semi-integrated bridge, presented in figure 9.9.

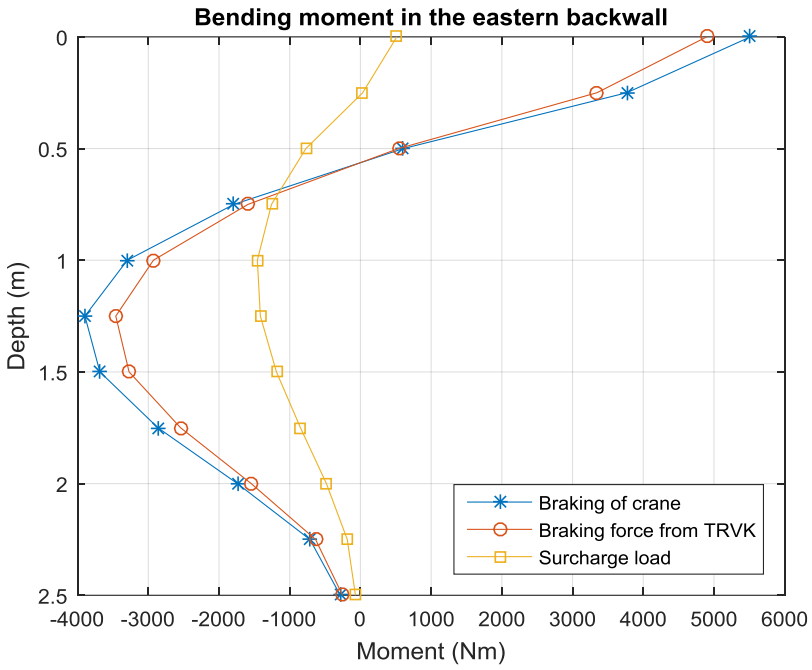

Figure 9.9. The bending moments of the eastern backwall (T4) plotted in the same figure for comparison.

9.3. Comparison of bending moments

The maximum bending moments of each load, for the two bridges and the cantilevering load case, at backwall T4 (the eastern backwall) is presented in table 9.2.

Table 9.2. Maximum bending moments in backwall T4 compared to those calculated for the cantilevering beam.

Load case	**Fully integrated**	**Semi-integrated**	**Cantilevering beam**
Temp. acc. to meas.	600,9 kNm	384,7 kNm	155,1 kNm
Temp. acc. to EC	1101,7 kNm	705,2 kNm	526,0 kNm
Brake acc. to meas.	5,3 kNm	5,5 kNm	28,4 kNm
Brake acc. to TRVK	4,7 kNm	4,9 kNm	32,1 kNm
At rest earth pressure	2,7 kNm	28,5 kNm	34,5 kNm
Surcharge load	1,7 kNm	1,5 kNm	15,5 kNm

It is noticeable how the FE model gives lower values of the bending moments of all the loads except the temperature movement. These results though are not fully comparable due to the deviation of the soil stiffness. A relatively large discrepancy is the difference between the bending moment due to the at rest earth pressure of the fully integrated and the semi-integrated bridge.

9.4. Comparison of fully integrated and semi-integrated backwall

The bending moments and the displacements, at the eastern backwall of the two bridges, are plotted for comparison in figures 9.10 and 9.11.

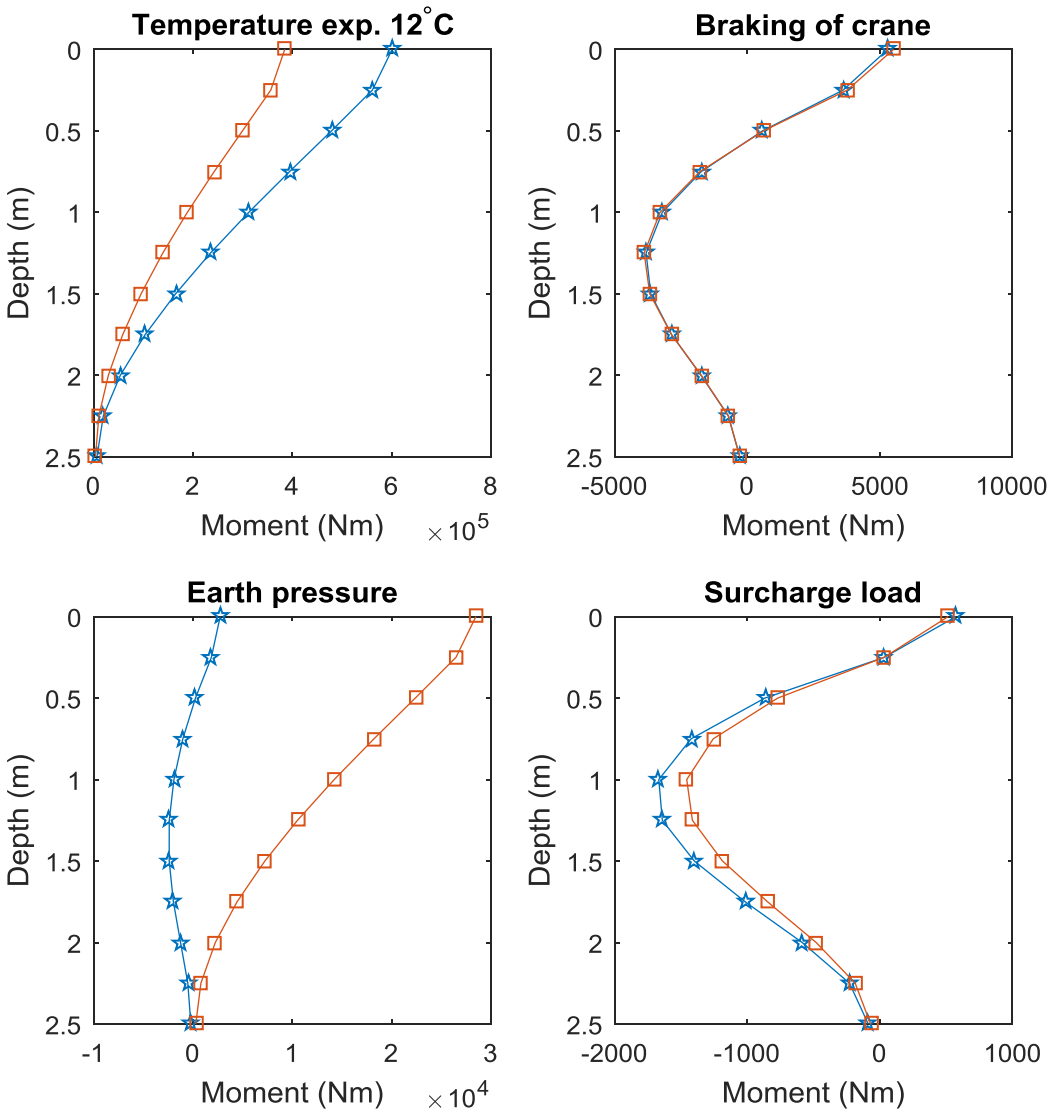

Figure 9.10. Comparison between the bending moments in the backwalls of the two bridge types. The line with stars represents the fully integrated bridge and the squared line represents the semi-integrated bridge.

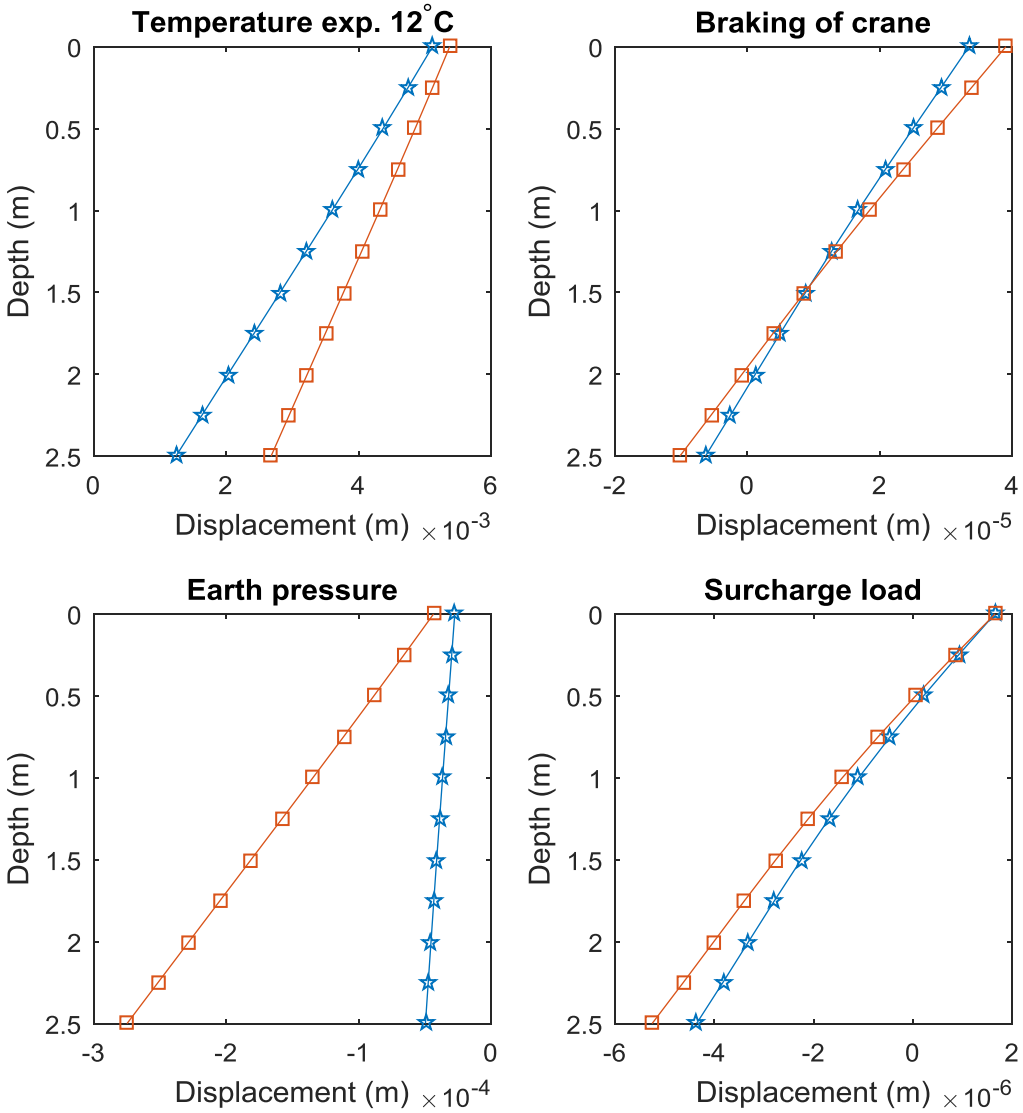

Figure 9.11. Comparison between the displacements of the backwalls of the two bridge types. The line with stars represents the fully integrated bridge and the squared line represents the semi-integrated bridge.

The bending moments are very alike, and the displacements differ mostly at the bottom of the backwall, where the displacements of the fully integrated bridge is lower due to the effect of the pile.

10. CONCLUSIONS

The derivation of the soil stiffness due to the measurement data did not provide satisfactory results, to prove either that a method of finding the real response of the soil structure interaction is possible or not. The deviation of the resulting stiffness and the predicted stiffness were too large. It should however be highlighted that the results point in a direction such as that the method of modelling the surface between the soil and the structure as linear springs could be made to work very efficiently with design of backwalls.

In the iteration method presented in the dissertation, the stiffness at one side is set constant and the stiffness at the other is increased. In reality, for the braking load, the abutment at the side which the braking load is directed at is exposed to a passive earth pressure and the other side is exposed to an active earth pressure. This will lead to a case were the passive side have increasing stiffness and the active side have decreasing stiffness. For the temperature expansion however, both of the abutments are exposed to passive earth pressure due to expanding movement of the bridge. This will lead to increasing earth pressure at both sides. For the iteration of the stiffness due to the temperature change, an alternative procedure where both sides were increased was tested, but did not provide better results.

The results showed that sufficient use of the soil structure interaction and the real response of the structures movements due to horizontal loading can be used to get smaller amount of reinforcement, and thus lighter and more material efficient structures. The results also show that the displacement mode of the backwall tends to be a mix of translation and rotation, with the translation being the dominant part. The rotation will however cause both active and passive earth pressure on the backwall, and since the rotation does not only happen in the base of the backwall, but in some cases in point somewhere on the wall, the use of Coloumb and Rankine theory is in some sense too conservative.

The large discrepancy between the bending moment given by the FE model and the ones given by the cantilevering load case is evidence of the advantages of using the spring boundary between the soil and structure.

No obvious conclusions can be drawn regarding what bridge type would be the best regarding deformations and earth pressures in the backwall, as the bending moments of the two types are very much alike for all the loads. Also the displacement at the backwall top, and thus the movement of the bridge slab, is in the same range. One explanation of the similar results can also be the application of the iterated soil stiffness on the semi-integrated bridge. The stiffness were iterated through measurements of a fully integrated bridge, and without knowledge of how the same loads would have affected a semi-integrated bridge.

10.1. Errors in the analysis

The discrepancy of the results can be explained by the uncertainties regarding the earth pressure on the "active earth pressure side", i.e. the side of the bridge from where the braking crane came from. This side was set constant during the iterations, but in reality the earth pressure behaves in a more decreasing way. It is however very hard to determine the exact behaviour of the earth pressure at this side. Same goes for the passive side, where the stiffness, and thus the earth pressure, was modelled with a linear increase with depth. This is a good enough assumption, but in reality the earth pressure vary linearly down to a certain depth, then to become constant during the rest.

There are also some uncertainties regarding the measurement data, as the results of the earth pressure change in the gauges where inconsistent and largely varying. At the same time, the earth pressure increase due to the braking crane where only measured in one point on the backwall.

Lastly, the approach of founding the soil stiffness solely on earth pressure difference and displacement in one point, which is not even the same point, is probably a too good simplification.

10.2. Further research

To continue the investigations on however the approach of modelling the surface between the soil and the structure as linear springs is applicable, here follows some suggestions on what to consider in future analysis.

- Evaluate what happens on the side of the bridge exposed to the active earth pressure
- Investigate how another distribution of the earth pressure/earth pressure coefficient, or another distribution of the soil stiffness, affect the outcome of the displacements
- Use of other measurement data/better measurement points can probably contribute to a better result. Measurement of a semi-integrated bridge should also be made in order to evaluate this particular type through measurement data as well.

BIBLIOGRAPHY

Bayoglu Flener, E., 2004. *Soil-Structure Interaction for Integral Bridges and Culverts,* Stockholm: Royal Institute of Technology (KTH), Sweden.

Bloodworth, A. G., Xu, M., Banks, J. R. & Clayton, C. R. I., 2012. Predicting the Earth Pressure on Integral Bridge Abutments. *Journal of Bridge Engineering,* 17(2), pp. 371-381.

Burström, P. G., 2007. *Byggnadsmaterial (In Swedish).* 2nd ed. Lund: Studentlitteratur.

Carlstedt, E., 2008. *Soil-Structure Interaction for Bridges with Backwalls,* Stockholm: Royal Institute of Technology (KTH), Sweden.

Chapelle, D. & Bathe, K.-J., 2011. *The Finite Element Analysis of Shells - Fundamentals.* 2nd ed. Berlin: Springer.

European Committee of Standardization, 2002a. *SS-EN 1990, Eurocode 0: Basis of Structural Design.* Stockholm: Swedish Standards Institute, Sweden.

European Committee of Standardization, 2003a. *SS-EN 1991-1-5, Eurocode 1: Actions on Structures- Part 1-5: General Actions- Thermal Actions.* Stockholm: Swedish Standards Institute, Sweden.

European Committee of Standardization, 2005b. *SS-EN 1992-2, Eurocode 2: Design of Concrete Structures- Part 2: Concrete Bridges- Design and Detailing Rules.* Stockholm: Swedish Standards Institute, Sweden.

Fartaria, C., 2012. *Soil-Structure Interaction in Integral Abutment Bridges,* Lisbon: Instituto Superior Téchnico, Universidade Téchinca de Lisboa, Portugal.

Getachew, A., 2003. *Traffic Load Effects on Bridges,* Stockholm: Royal Institute of Technology (KTH), Sweden.

Hassiotis, S. & Xiong, K., 2007. *Deformation of Cohesionless Fill Due to Cyclic Loading,* Hoboken, New Jersey: Department of Civil, Environmental and Ocean Engineering - Stevens Institute of Technology.

Highways Agency, 2003. *BA 42/96 The Design of Integral Bridges,* United Kingdom: The Stationary Office.

James, G., 2003. *Analysis of Traffic Load Effect on Railway Bridges,* Stockholm: Royal Institute of Technology (KTH), Sweden.

Karlsson, D. & Welinder, N., 2011. *Metod för parametrisering av brokonstruktioner (In Swedish),* Lund: Lund University of Technology, Sweden.

Karoumi, R. et al., 2007. *Modern mät- och övervakningsmetodik för bedömning av befintliga broar (In Swedish),* Stockholm: Royal Institute of Technology (KTH).

Kerokoski, O., 2006. *Soil-Structure Interaction of Long Jointless Bridges with Integral Abutments,* Tampere: Tampere University of Technology, Finland.

Krenk, S., 2009. *Non-Linear Modelling and Analysis of Solids and Structures.* Cambridge: Cambridge University Press.

Laaksonen, A., 2011. *Structural Behaviour of Long Concrete Integral Bridges,* Tampere: Tampere University of Technology, Finland.

Larsson, C. & Svensson, G., 2013. *Realistic Modeling of Thermal Effects in Concrete Bridges,* Lund: Lund University of Technology, Sweden.

Larsson, O., 2012. *Climate Related Thermal Actions for Reliable Design of Concrete Structures,* Lund: Lund University of Technology, Sweden.

Lemnitzer, A. et al., 2009. Lateral Performance of Full-Scale Bridge Abutment Wall with Granular Backfill. *Journal of Geotechnical and Geoenvironmental Engineering,* 135(4), pp. 506-514.

Lock, R., 2002. *Integral Bridge Abutment,* Cambridge: University of Cambridge, United Kingdom.

Malerba, P. G. & Comatia, G., 2014. Desgin and Construction of Two Integral Bridges for the Runway of Milan Malpensa Airport. *Structure and Infrastructure Engineering,* 11(4), pp. 486-500.

Mårtensson, A. & Isaksson, T., 2010. *Byggkonstruktion - Regel- och formelsamling (In Swedish).* 2:5 ed. Lund: Studentlitteratur.

Olmo Segovia, A., 2006. *FEM Simulation of a Steel Box Culvert Test,* Stockholm: Royal Institute of Technology (KTH), Sweden.

Ottosen, N. & Petersson, H., 1992. *Introduction to the Finite Element Method.* Harlow: Pearson Prentice Hall.

Pétursson, H., 2000. *Broar med integrerade landfästen (In Swedish),* Luleå: Luleå University of Technology, Sweden.

Pétursson, H., 2015. *Design of Steel Piles for Integral Abutment Bridges,* Luleå: Luleå University of Technology, Sweden.

Rajeev, P. et al., 2014. *Earth Pressure Development in Integral Abutment Bridge subjected to Thermal Loadings.* Melbourne, 8th Australasian Congress on Applied Mechanics, ACAM 8.

Rylander, P. E., 2006. *Dynamic Effects Generated by Trains on Railway Bridges,* Lund: Lund University of Technology, Sweden.

Salman, F. A., Al-Shakarchi, Y. J., Husain, H. M. & K., S. D., 2010. Distribution of Earth Pressure Behind Retianing Walls Considering Different Approaches. *International Journal of the Physical Sciences,* 5(9), pp. 1389-1400.

Scanscot Technology, 2015. *Brigade Plus User´s Manual version 6.1.* Sweden: Scanscot Technology.

Sundquist, H., 2009. *Infrastructure Structures.* 2nd ed. Stockholm: Royal Institute of Technology (KTH), Sweden.

Swedish Road Administration, 1996. *Broprojektering - en handbok (In Swedish).* Borlänge: Swedish Road Administration.

Swedish Road Administration, 2011a. *TK Geo (In Swedish).* Borlänge: Swedish Road Administration.

Swedish Road Administration, 2011b. *TRVK Bro 11 (In Swedish).* 2011:085 ed. Borlänge: Swedish Road Administration.

Sällfors, G., 2009. *Geoteknik - Jordmateriallära (In Swedish).* Göteborg: s.n.

Timoshenko, S. & Goodier, J., 1951. *Theory of Elasticity.* 2nd ed. New York: McGraw-Hill.

Wendner, R., Strauss, A. & Bergmeister, K., 2011. Jointless Bridges - Performance Assessment of Soil-Structure Interaction. In: K. Nishijima, ed. *Applications of Statistics and Probability in Civil Engineering.* London: Taylor & Francis Group, pp. 1069-1076.

White, H., Petursson, H. & Collin, P., 2010. Integral Abutment Bridges: The European Way. *Practice Periodical on Structural Design and Construction,* 15(3), pp. 201-208.

Zhang, J.-M., Shamoto, Y. & Tokimatsu, K., 1998. Evaluation of Earth Pressure Under Any Lateral Deformation. *Soils and Foundations,* Volume 38, pp. 15-33.

APPENDIX A Loading test crane

5.10.05

TAMPEREEN TEKNILLINEN YLIOPISTO

Koekuormitusohjelma Haavistonjoen sillalle

1. Silta ja sen sijainti

Koekuormitettava silta on Haavistonjoen silta. Silta sijaitsee VT 9:llä noin 5 kilometriä Orivedeltä Jyväskylän suuntaan. Sillalla ajoradan leveys on 11.0 m.

2. Koekuormitusajankohta

Koekuormitusajankohta valitaan tarkasti lähempänä koekuormitusajankohtaa. Koekuormitusajankohta riippuu siitä onko tie jäässä ja sataako mahdollisesti lunta. Koekuormitus on tarkoitus järjestää lokakuun kahden ensimmäisen viikon aikana joko 6.10, jos olosuhteet ovat hyvät tai 13.10, jos tie on pahasti jäässä 6.10. Koekuormitus kestää yhden päivän.

3. Koekuormittava ajoneuvo

Koekuormittava ajoneuvo on 4-akselinen nosturi, kokonaispainoltaan 60 tonnia. Nosturi on varustettu ABS-jarruin. Nosturi on tyypiltään: Liebherr LTM 1090, katso kuva 3.1. Huippunopeus on 80 km/h. Hämeen tiepiiriltä anotaan lupa kyseisen nosturin käyttämiselle.

Kuva 3.1 Koekuormittava ajoneuvo, johon on kiinnitetty nopeuden mittalaite

APPENDIX B Finnish national annex chapter 6

ANNEX 6

NATIONAL ANNEX

TO STANDARD

SFS-EN 1991-1-5 EUROCODE 1: ACTIONS ON STRUCTURES

Part 1-5: General actions. Thermal actions

Preface

This National Annex is used together with standard SFS-EN 1991-1-5:2004.

This National Annex sets out the national parameters for the following paragraphs in standard EN 1991-1-5 concerning buildings where national selection is permitted.

- 5.3(2) (Tables 5.1, 5.2 and 5.3)
- A.1(1)
- A.1(3)
- A.2(2)

5.3 Determination of temperature profiles

5.3(2) (Tables 5.1, 5.2 and 5.3)

Table 5.1 Indicative temperatures of inner environment T_{in}

T_1= 25 ºC (summer) and T_2= 23 ºC (winter) are used as temperature values T_1 and T_2.

Table 5.2 Indicative temperatures T_{out} for buildings above ground level

Temperature values specified in isotherm maps, set out in Annex A hereunder, are used for the maximum shade air temperature T_{max} and the minimum shade air temperature $T_{min.}$

For values of solar radiation effects T_3, T_4 and T_5 in summer, T_3= 5 ºC, T_4= 10 ºC and T_5= 15 ºC are used for structural elements facing north and east, and T_3= 10 ºC, T_4= 20 ºC and T_5= 30 ºC for structural elements facing south and west or for horizontal structural elements.

Table 5.3 Indicative temperatures T_{out} for underground parts of buildings

T_6 = 6 ºC, T_7 = 4 ºC, T_8= -7 ºC and T_9= -4 ºC are used as temperature values of T_6, T_7, T_8 and T_9.

Annex A
Isotherms of national minimum and maximum shade air temperatures

A.1 General

A.1(1)

The minimum shade air temperatures and the maximum shade air temperatures represent values with an annual probability of being exceeded of 0.02.

Data (isotherm maps) on annual minimum and maximum shade air temperatures is shown in Figures 1 and 2.

Shade air temperature values are adapted in accordance with the altitude above sea level by deducting 0.5°C per altitude difference of 100 m in respect of the minimum shade air temperature, and 1.0 °C per altitude difference of 100 m in respect of the maximum shade air temperature.

A. 1(3)

Unless other data is available, the value of 10ºC is used for the initial temperature T_0.

A.2 Maximum and minimum shade air temperature values with an annual probability of being exceeded p other than 0.02

A.2(2)

The mathematical method, set out in paragraph A.2(2), may be used to determine the annual maximum or minimum shade air temperature value. Then the maximum and minimum temperature values are determined directly from the statistics, and the coefficients k_1, k_2, k_3 and k_4 are derived through them. No values are given for coefficients in this National Annex.

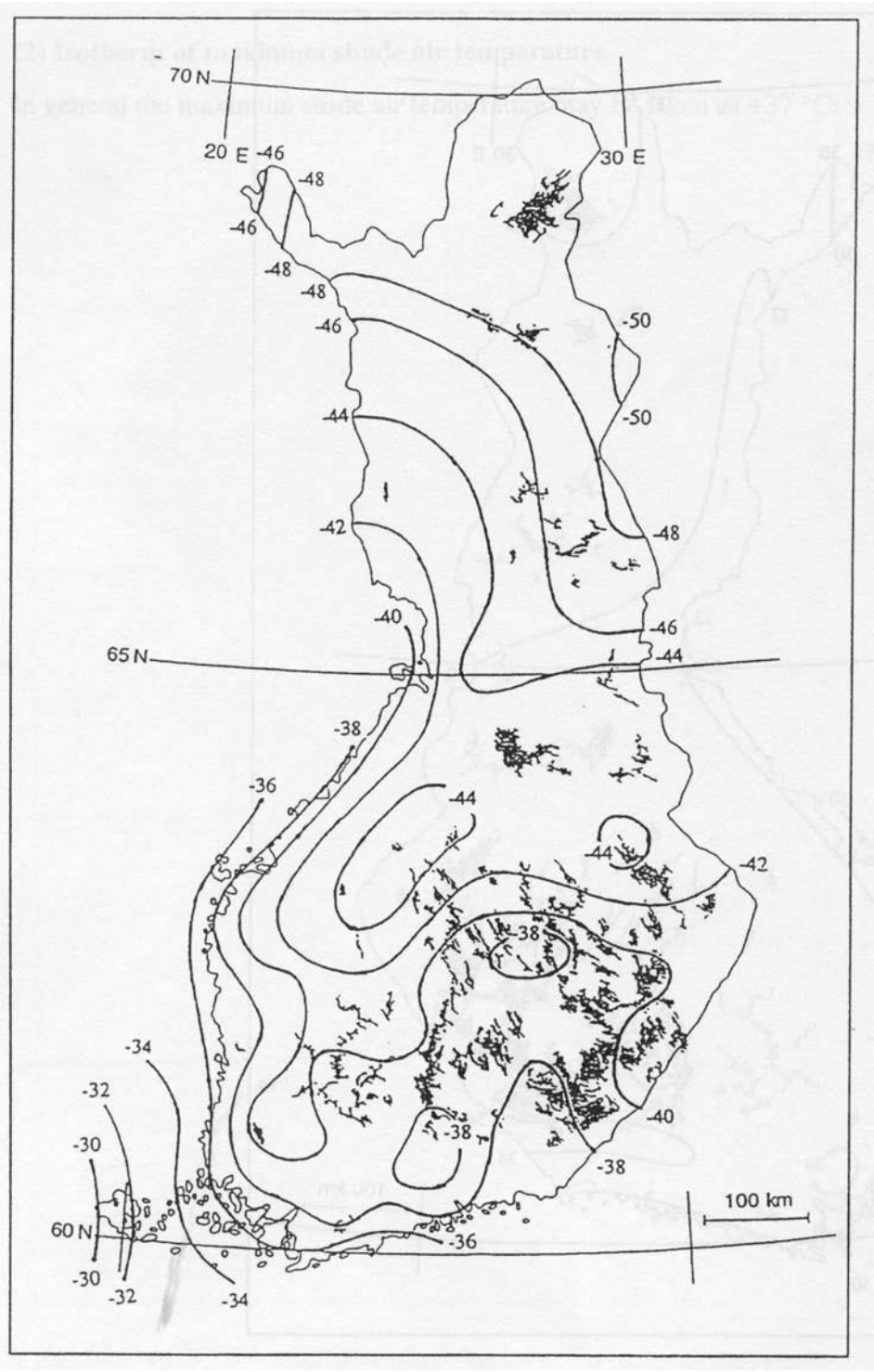

Figure 1 Isotherms of minimum shade air temperature (^{o}C). There may be considerable local deviations depending on the topography and built environment.

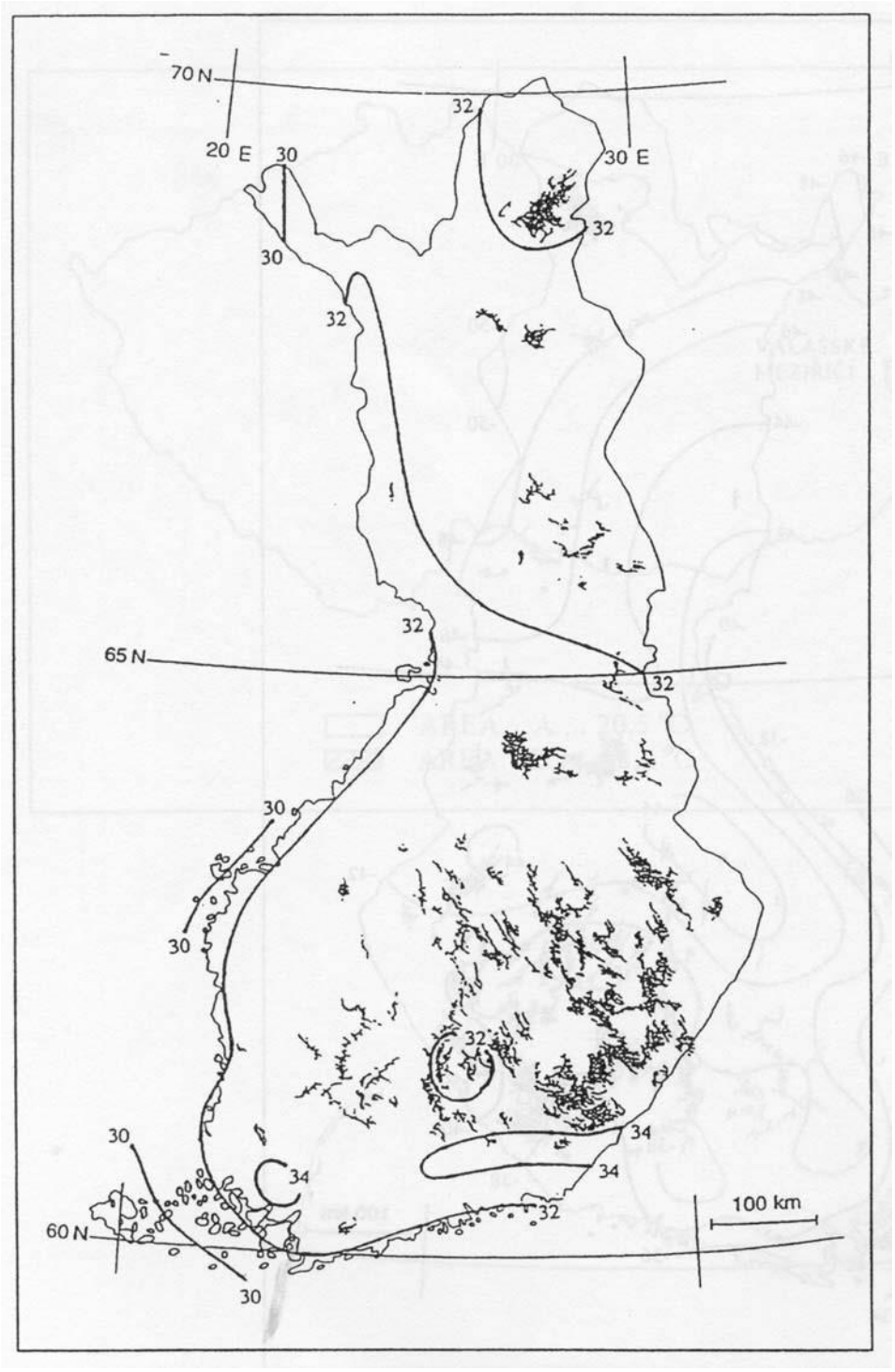

Figure 2 Isotherms of maximum shade air temperature (°C). There may be considerable local deviations depending on the topography and built environment.

APPENDIX C Calculations

Bridge geometries

$Lb := 51.2$

$Hbw := 2.5$

$Bb := 11.5$

Material properties

$\gamma c := 24 \cdot 10^{3}$

$\alpha\Delta T := 10 \cdot 10^{-6}$

Soil properties

$\gamma bf := 20 \cdot 10^{3}$

$\phi := 42 \cdot \frac{\pi}{180}$

$Katrest := 1 - \sin(\phi)$

$Katrest = 0.331$

$Kp := \left(\tan\left(45 \cdot \frac{\pi}{180} + \frac{\phi}{2}\right)\right)^{2}$

$Kp = 5.045$

Braking force

$iterationstep := \frac{\left(470 \cdot 10^{3} - 170 \cdot 10^{3}\right)}{(170 - 40)}$

Lengths and forces from TDOK 2013:0273

$increase := (Lb - 40) \cdot iterationstep$

$FB := 170 \cdot 10^{3} + increase$

$FB = 1.958 \times 10^{5}$

Distributed braking force

$qB := \frac{FB}{Bb}$

$qB = 1.703 \times 10^{4}$

Braking of the crane

$v := 16.2$

$v0 := 0$

$t := 9.6$

$t0 := 5.2$

$$a := \frac{(v - v0)}{(t - t0)}$$

$a = 3.682$

$mass\_crane := 60000$

$Fcrane := mass\_crane \cdot a$

$Fcrane = 2.209 \times 10^{5}$

$$qBcrane := \frac{Fcrane}{(Bb)}$$

$qBcrane = 1.921 \times 10^{4}$

Temperature

$TmaxEC := 32$

Temperatures from Finnish NA

$T0 := 10$

$\Delta T\_EC := TmaxEC - T0$

$\Delta T\_EC = 22$

$\varepsilon\Delta T\_EC := \Delta T\_EC \cdot \alpha\Delta T$

$\varepsilon\Delta T\_EC = 2.2 \times 10^{-4}$

$$\delta T\_EC := \varepsilon\Delta T\_EC \cdot \frac{Lb}{2}$$

$\delta T\_EC = 5.632 \times 10^{-3}$

Limit value displacement

$$lim := \frac{Hbw}{200}$$

Limit value from TDOK 2013:0273

$lim = 0.013$

The displacement $0 < \delta T,EC < Hbw/200$

$Tmax := -2$

Temperatures from measurements

$Tmin := -14$

$\Delta T := Tmax - Tmi$

$\Delta T = 12$

$\varepsilon\Delta T := \Delta T \cdot \alpha\Delta T$

$\varepsilon\Delta T = 1.2 \times 10^{-4}$

$$\delta T := \varepsilon\Delta T \cdot \frac{Lb}{2}$$

$\delta T = 3.072 \times 10^{-3}$

The displacement $0 < \delta T < Hbw/200$

Surcharge load

$qSL := 15 \cdot 10^{3}$

From TRVK

Earth pressure due to at rest earth pressure

$$pbf := Katrest \cdot \gamma bf \cdot Hbw$$

$$pbf = 1.654 \times 10^{4}$$

Earth pressure due to braking force

$$pB := \frac{(2 \cdot qB)}{Hbw}$$

$$pB = 1.362 \times 10^{4}$$

$$pB\_crane := \frac{(2 \cdot qBcrane)}{Hbw}$$

$$pB\_crane = 1.537 \times 10^{4}$$

Earth pressure due to temperature change

$$pT := \left[Katrest + \delta T \cdot \frac{200}{Hbw} \cdot (Kp - Katrest) \right] \cdot \gamma bf \cdot Hbw$$

From TDOK 2013:0273

$$pT\_EC = 2.522 \times 10^{5}$$

$$pT\_EC := \left[Katrest + \delta T\_EC \cdot \frac{200}{Hbw} (Kp - Katrest) \right] \cdot \gamma bf \cdot Hbw$$

From TDOK 2013:0273

$$pT\_EC = 1.227 \times 10^{5}$$

Earth pressure due to surcharge load

$$pSL := qSL \cdot Katrest$$

$$pSL = 4.963 \times 10^{3}$$

Bending moment in the top of the backwall

Earth pressure

$$Mbf := \frac{\left(pbf \cdot Hbw^2\right)}{3}$$

$$Mbf = 3.447 \times 10^4$$

Braking force

$$MB := \frac{\left(pB \cdot Hbw^2\right)}{3}$$

$$MB = 2.838 \times 10^4$$

$$MB\_crane := \frac{\left(pB\_crane \cdot Hbw^2\right)}{3}$$

$$MB\_crane = 3.202 \times 10^4$$

Temperature

$$MT\_EC := \frac{\left(pT\_EC \cdot Hbw^2\right)}{3}$$

$$MT\_EC = 2.557 \times 10^5$$

$$MT := \frac{\left(pT \cdot Hbw^2\right)}{3}$$

$$MT = 1.551 \times 10^5$$

Surcharge load

$$MSL := \frac{\left(pSL \cdot Hbw^2\right)}{2}$$

$$MSL = 1.551 \times 10^4$$

Stiffness from measured earth pressures and displacements

Load case	**Earth pressure difference**	**Abutment displacement**
Temperature (T4)	86	5,3
Temperature (T1)	57,5	0,3
Braking (T4)	3	0,03

$pT4 := 86 \cdot 10^{3}$

$pT1 := 57.5\,10^{3}$

$pBT4 := 3 \cdot 10^{3}$

$\delta T4 := 5.3\,10^{-3}$

$\delta T1 := 0.3\,10^{-3}$

$\delta BT4 := 0.03\,10^{-3}$

$kT4 := \frac{pT4}{\delta T4}$

$kT1 := \frac{pT1}{\delta T1}$

$kBT4 := \frac{pBT4}{\delta BT4}$

$kT4 = 1.623 \times 10^{7}$ Stiffness k=16,2 MN/m/m^2

$kT1 = 1.917 \times 10^{8}$ Stiffness k=192 MN/m/m^2

$kBT4 = 1 \times 10^{8}$ Stiffness k=100 MN/m/m^2

APPENDIX D Results of bending moments

D1 Haavistonjoki Bridge (fully integrated bridge)

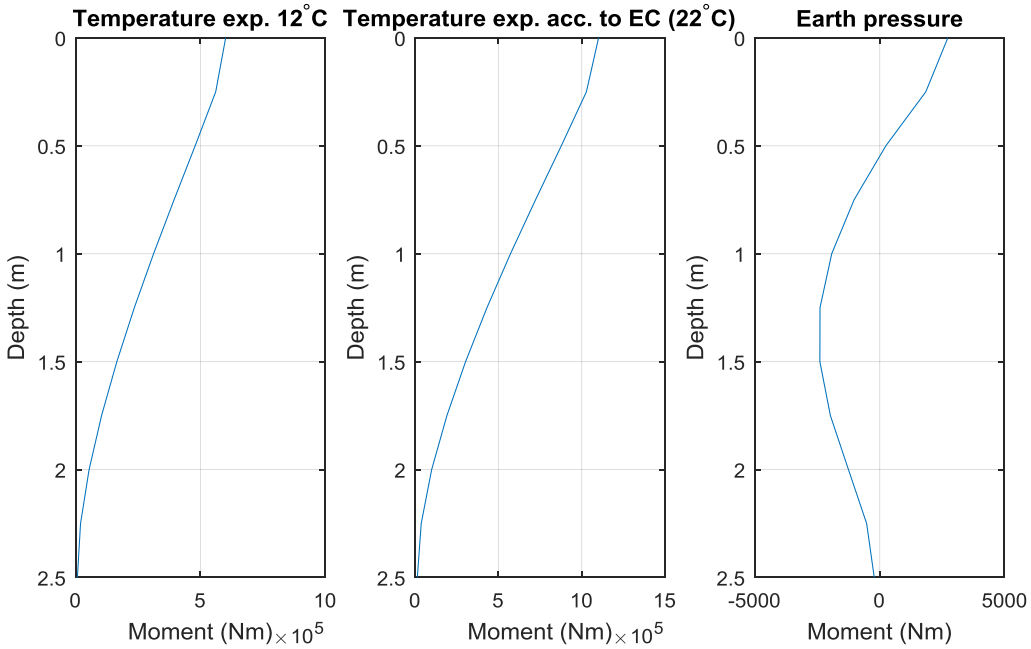

Figure D.1. Bending moments in the eastern abutment (T4). The left curve is the moment due to the temperature difference from the measurements, the middle curve is the moment due to the temperature difference given in Eurocode at the location of Tampere and the right curve is the moment due to the at rest earth pressure.

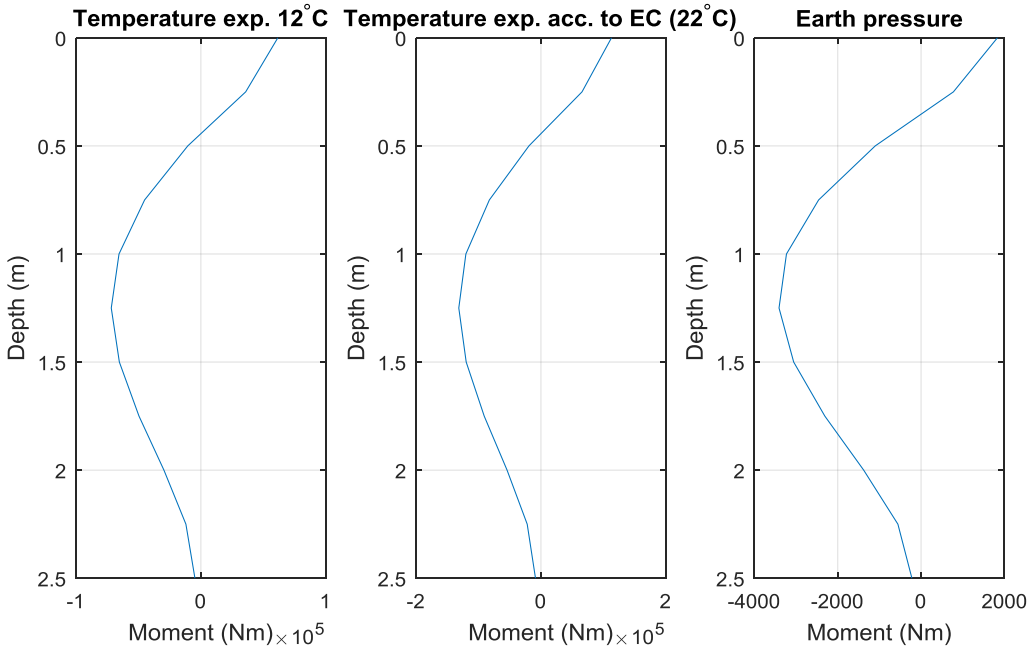

Figure D.2. Bending moments in the western abutment (T1). The left curve is the moment due to the temperature difference from the measurements, the middle curve is the moment due to the temperature difference given in Eurocode at the location of Tampere and the right curve is the moment due to the at rest earth pressure.

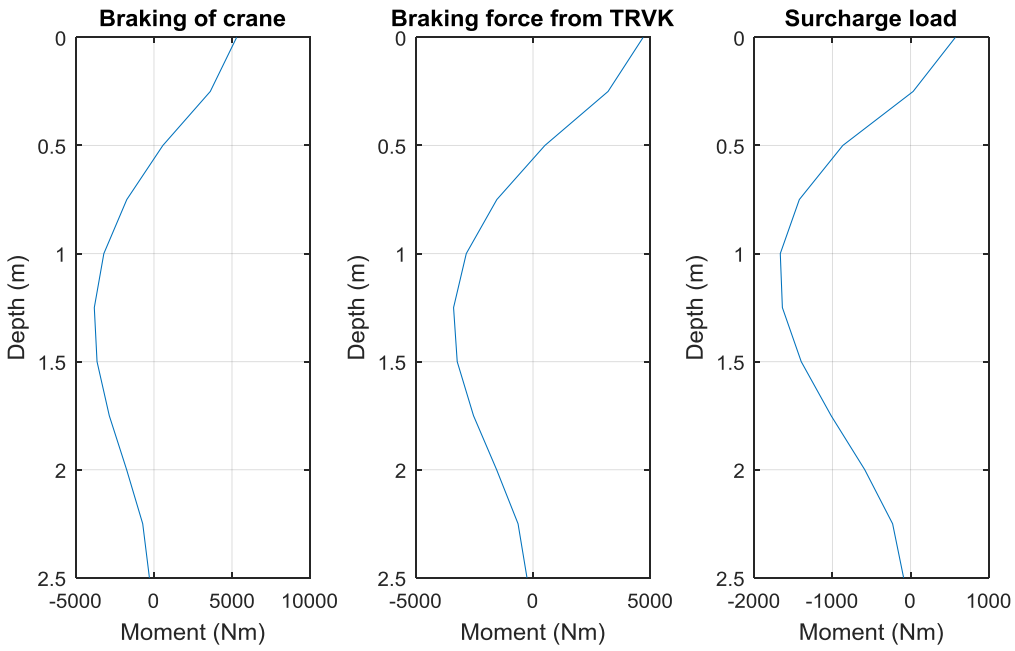

Figure D.3. Bending moments in the eastern abutment (T4). The left curve is the moment due to the braking of the crane, the middle curve is the moment due to the braking force given in TRVK and the right curve is the moment due to the surcharge load.

D2 Semi-integrated abutment bridge

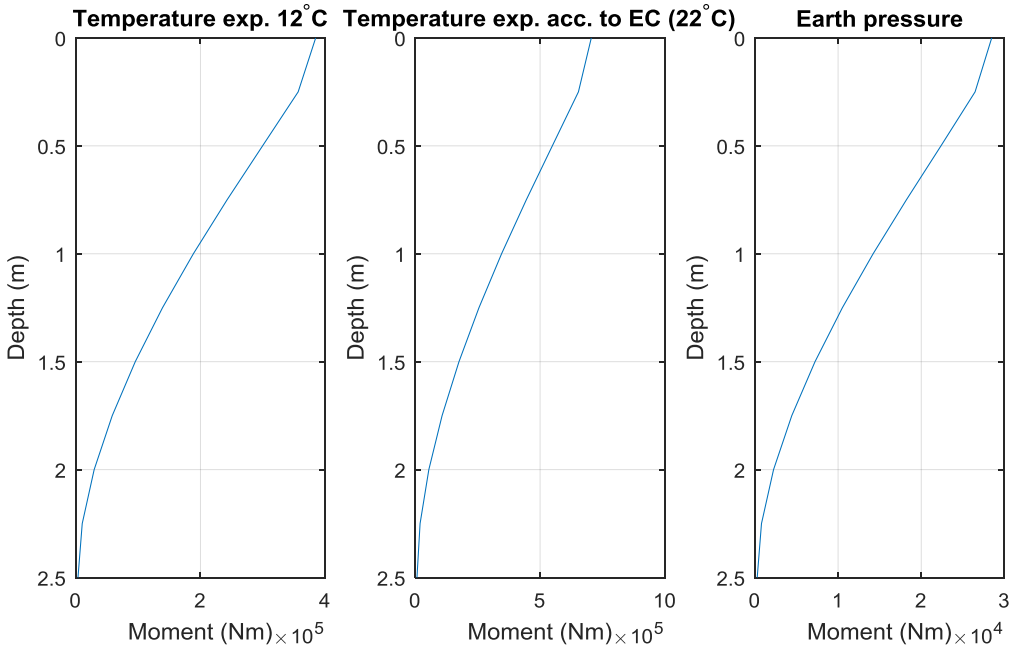

Figure D.4. Bending moments in the eastern abutment (T4). The left curve is the moment due to the temperature difference from the measurements, the middle curve is the moment due to the temperature difference given in Eurocode at the location of Tampere and the right curve is the moment due to the at rest earth pressure.

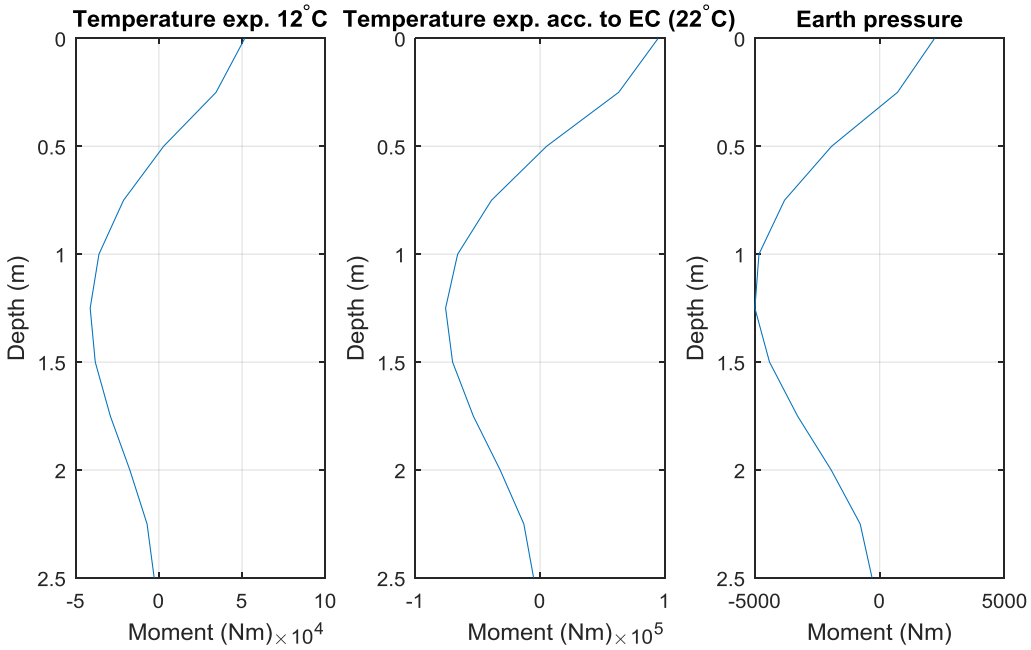

Figure D.5. Bending moments in the western abutment (T1). The left curve is the moment due to the temperature difference from the measurements, the middle curve is the moment due to the temperature difference given in Eurocode at the location of Tampere and the right curve is the moment due to the at rest earth pressure.

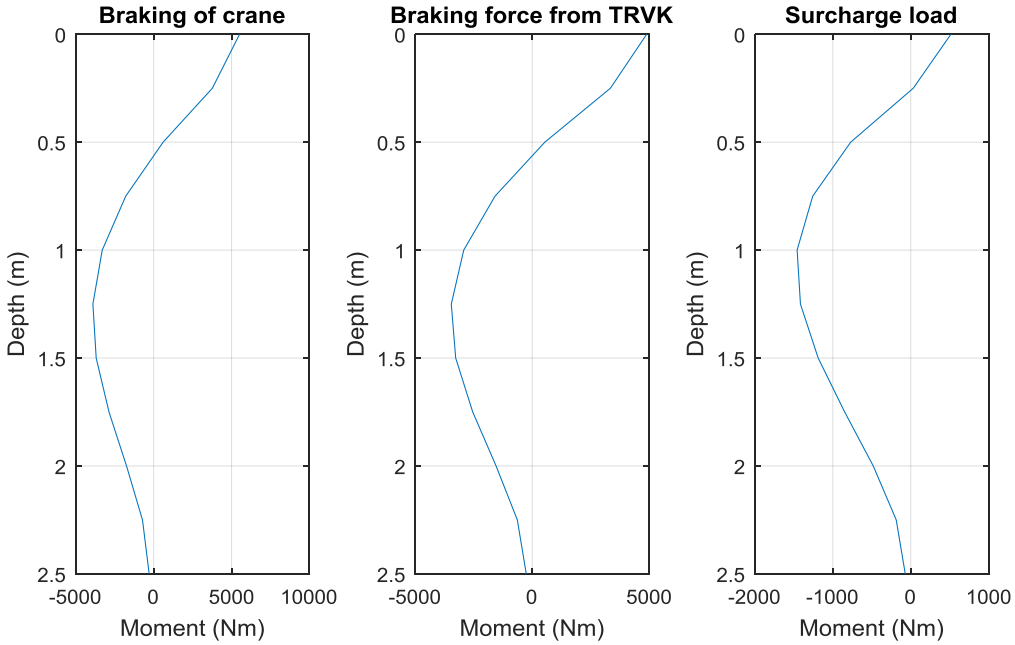

Figure D.6. Bending moments in the eastern abutment (T4). The left curve is the moment due to the braking of the crane, the middle curve is the moment due to the braking force given in TRVK and the right curve is the moment due to the surcharge load.